

KUL-TF-04/13  
 FT-UAM-04-05  
 IFT-UAM/CSIC-04-12

hep-th/0404055

# Getting just the Supersymmetric Standard Model at Intersecting Branes on the $\mathbb{Z}_6$ -orientifold

**Gabriele Honecker<sup>1</sup> and Tassilo Ott<sup>2</sup>**

<sup>1</sup> *Departamento de Física Teórica C-XI and Instituto de Física Teórica C-XVI,  
 Universidad Autónoma de Madrid, Cantoblanco, 28049 Madrid, Spain*  
 E-mail: gabriele@th.physik.uni-bonn.de

<sup>2</sup> *Institute for Theoretical Physics, KULeuven  
 Celestijnenlaan 200 D, 3001 Leuven, Belgium*  
 E-mail: tassilo.ott@fys.kuleuven.ac.be

## Abstract

In this paper, globally  $\mathcal{N} = 1$  supersymmetric configurations of intersecting D6-branes on the  $\mathbb{Z}_6$  orientifold are discussed, involving also fractional branes. It turns out rather miraculously that one is led almost automatically to just *one* particular class of 5 stack models containing the SM gauge group, which all have the same chiral spectrum. The further discussion shows that these models can be understood as exactly the supersymmetric standard model without any exotic chiral symmetric/antisymmetric matter. The superpartner of the Higgs finds a natural explanation and the hypercharge remains massless. However, the non-chiral spectrum within the model class is very different and does not in all cases allow for a  $\mathcal{N} = 2$  low energy field theoretical understanding of the necessary breaking  $U(1) \times U(1) \rightarrow U(1)$  along the Higgs branch, which is needed in order to get the standard Yukawa couplings.

Also the left-right symmetric models belong to exactly *one* class of chiral spectra, where the two kinds of exotic chiral fields can have the interpretation of forming a composite Higgs. The aesthetical beauty of these models, involving only non-vanishing intersection numbers of an absolute value three, seems to be unescapable.

# 1 Introduction

String Theory claims to be the correct unifying theory of gravity and elementary particle physics. As the latter, it should contain the standard model as a low energy limit, which is a chiral gauge theory. Since it was realized that chiral matter is possible in the context of intersecting D-branes [1], many different approaches have been taken, the most successful ones being constructions with intersecting D6-branes in type IIA orientifolds [2–13] (for recent reviews of the topic see [14–17]). The branes wrap special Lagrangian 3-cycles of the compact space in these models, which in general can be a simple toroidal, orbifolded or Calabi-Yau space, where the worldsheet parity symmetry  $\Omega$  together with a space time symmetry  $\mathcal{R}$  is modded out. In this picture, chiral fermions are localized at the intersections of the different stacks of D6-branes and consequently are 4-dimensional, whereas the gauge fields live on the whole worldvolume of the branes and by this are 7-dimensional. Finally, gravity is contained in the closed string sector of the theory and lives in the 10-dimensional bulk.

The massless chiral fermion spectrum can be determined in all three cases, as it only depends on the homology of the 3-cycles [18, 19]. On the other hand, the non-chiral part of the spectrum depends on the closed string moduli and requires the worldsheet CFT computation of the one loop amplitude that can be explicitly obtained only in the case of the torus or orbifolded torus. The 6-torus usually is assumed to be factorized in three 2-tori, i.e.  $T^6 = T^2 \times T^2 \times T^2$ . Every 3-cycle factorizes into three 1-cycles, one on every torus, and one obtains a nice geometrical picture.

In such an approach, a model containing only the standard model matter in the chiral sector has been obtained [20] (for similar subsequent models see [21, 22]). But shortly afterwards, it was realized that this model is unstable due to the uncancelled NS-NS-tadpoles becoming manifest in the runaway behavior of the complex structure and dilaton moduli [23, 24] (see also the remarks in [25]). The first instability can be cured by making the transition to a  $\mathbb{Z}_3$ -orientifold (where the exact realization of the standard model is different), but the dilaton instability cannot. Although this instability might be interesting from the perspective of cosmology and particularly inflation at first sight, it has been found, that only under very special and rather unsatisfactory requirements (for instance some moduli have to be fixed by an unknown mechanism), the remaining modulus could act as the inflaton [26] (for a different approach see e.g. [27]). Beside that fact, inflation has to end and today only a very small cosmological constant is observed, which would require a very unnatural fine-tuning to comply with a natural timescale of for instance the dilaton instability.

Therefore, in the recent past another road has mainly been taken, namely the attempt to construct instead a  $\mathcal{N} = 1$  supersymmetric standard model (or supersymmetric  $SU(5)$  GUTs and Pati-Salam models respectively). This goal so far has been achieved only with moderate success: either the constructions are plagued with a large amount of exotic chiral matter, as in the  $\mathbb{Z}_2 \times \mathbb{Z}_2$  orientifold of [28–35] or brane recombinations of non-Abelian gauge groups are needed, as in the  $\mathbb{Z}_4$  orientifold of [36] or the  $\mathbb{Z}_4 \times \mathbb{Z}_2$  [37, 38], giving rise to Pati-Salam-Models, and leading to non-flat and non-factorizable branes which give up the complete predictability of the worldsheet CFT approach. Another possibility are the constructions of [39, 40], where only the sectors between certain branes are locally  $\mathcal{N} = 1$ -supersymmetric (Q-SUSY theories), but the setting as a whole is not, meaning that the NS-NS-tadpole is not cancelled. For similar constructions see [41, 42].

If a realistic globally  $\mathcal{N} = 1$  supersymmetric standard model with the right chiral spectrum was found, many phenomenological properties could be discussed [43], such as for instance

proton decay [44] or the running of the gauge couplings [45, 46] and a possible gauge unification [47], the generation of masses [48–50] and the precise realization of the Higgs mechanism(s) [51], leading towards the goal of making contact with experimental reality [52]. It could even lead to an understanding of supersymmetry breaking [53, 54].

Such a model can be compared to the minimal supersymmetric standard model (MSSM), which is claimed to be the best candidate for the search for supersymmetry at the LHC (for a good review see for instance [55]). This model has more predictive properties than a general supersymmetric standard model, it contains only a minimal Higgs sector of two  $SU(2)$  doublets and their superpartners whose hypercharge is exactly opposite, the declaration that all scalar masses are the same, all gaugino masses are the same, some statements about soft supersymmetry breaking (in the context of intersecting branes see [54]). In the past, the term MSSM often has been used very sloppy within string model building, basically meaning only the correct chiral spectrum. For a recent overview about the actual status of D6-brane constructions see [56, 57].

A new possibility that has been explored is to get chiral supersymmetric standard-like models in a completely different corner of Calabi-Yau moduli space, namely at the Gepner points [58–61] (for an introduction see [62]).

In this paper, the aim of getting a precise realization of a supersymmetric standard model will be continued furthermore on the compact space  $T^6/\mathbb{Z}_6$ , which again corresponds to a  $\mathcal{N} = 2$  background of type II theory, following the classification of orbifolds in [63, 64]. For this background (which geometrically can be defined in two different consistent ways on the 2-tori  $T_k^2$ ), the  $\mathbb{Z}_2$ -twisted sector in both cases contributes a non-vanishing number  $h_{2,1}$  to the number of complex structure deformations and so contains twisted 3-cycles, requiring the introduction of fractional branes [65, 66], similar to the  $\mathbb{Z}_4$ -orientifold of [36].

The organization of the paper is as follows. The geometry of the orbifold is discussed in detail in section 2, including the definition of bulk and fractional cycles and an integral basis of homology, the orientifold plane and the resulting R-R-tadpole conditions for all possible choices of **A**- and **B**-tori<sup>1</sup>. Finally, the conditions for  $\mathcal{N} = 1$  supersymmetry on the bulk and exceptional cycles are derived.

Section 3 discusses the calculation of the one-loop amplitudes and the transformation to the tree-channel, preparing the calculation of the chiral and non-chiral open string spectrum.

Subsequently, there is a detailed discussion on anomalies and the generalized Green-Schwarz mechanism in section 4.

In section 5, we finally come to the search of phenomenologically interesting models with a different number of stacks, leading to a detailed presentation of the explicit supersymmetric standard model which we have found in section 6. There is also a short discussion on another possible left/right symmetric model in section 7.

The conclusions and prospects are given in chapter 8.

Some technical details are collected in appendices A to D.

---

<sup>1</sup>They correspond to a vanishing or non-vanishing NS-NS 2-form flux  $b$  in the T-dual F-flux picture of D9-branes.

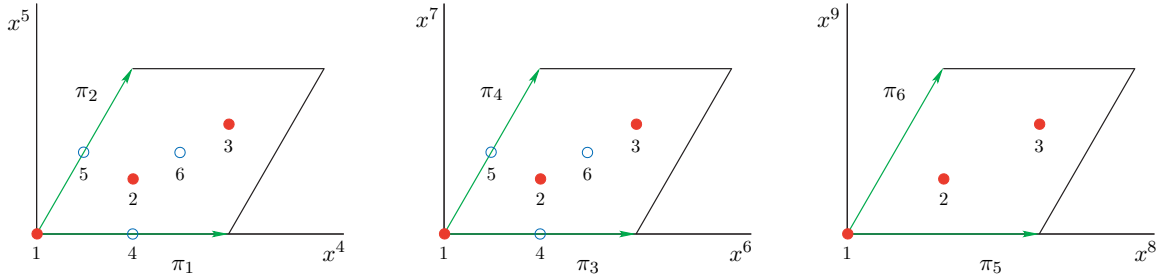


Figure 1: Fixed points of the  $T^6/\mathbb{Z}_6$  orbifold. Full circles denote  $\theta^2$  fixed points on  $T_1^2 \times T_2^2$ , empty circles additional  $\theta^3$  fixed points. On  $T_3^2$ , the points 1,2,3 are fixed under  $\theta$ , the whole  $T_3^2$  is fixed under  $\theta^3$ . The coordinates are depicted for the **AAA** torus.

## 2 Geometry of the $T^6/\mathbb{Z}_6$ orbifold

If one assumes a factorization of the  $T^6$  into three 2-tori, then the  $T^6/\mathbb{Z}_6$  orbifold is generated by a rotation  $\theta$  of the form

$$\theta : \quad z^k \rightarrow e^{2\pi i v_k} z^k \quad \text{for } k = 1, 2, 3 \quad (1)$$

where the shift vector  $v$  is given by  $v = (1/6, 1/6, -1/3)$ , see for instance [63, 64], and  $z^k$  is the complex coordinate on  $T_k^2$ .<sup>2</sup>

Apart from the  $\mathbb{Z}_6$  fixed points, additional points are fixed under the  $\mathbb{Z}_3$  subsymmetry generated by  $\theta^2$ . At all these fixed points, exceptional 2-cycles of zero volume<sup>3</sup> are stuck. Under the  $\mathbb{Z}_2$  subsymmetry generated by  $\theta^3$ , the whole third 2-torus  $T_3^2$  is fixed, and exceptional 3-cycles which are products of 2-cycles stuck at the  $\mathbb{Z}_2$  fixed points on  $T_1^2 \times T_2^2$  times 1-cycles on the fix-torus  $T_3^2$  appear. The geometry is depicted in figure 1.

The Hodge numbers of the  $\mathbb{Z}_6$  orbifold are as follows (see e.g. [4] for the closed string spectrum, [69] for the number of untwisted and twisted moduli and [70] for the hodge numbers explicitly),

$$\begin{aligned} h_{1,1}^U &= 5, & h_{1,1}^\theta &= 3, & h_{1,1}^{\theta^2} &= 15, & h_{1,1}^{\theta^3} &= 6, \\ h_{2,1}^U &= 0, & h_{2,1}^\theta &= 0, & h_{2,1}^{\theta^2} &= 0, & h_{2,1}^{\theta^3} &= 5. \end{aligned} \quad (2)$$

In the following, we will only consider the 3-cycles, but not the 2-cycles, since only intersections of D6-branes wrapping different 3-cycles in the compact dimensions give rise to chiral fermions. According to the value of the third Betti number,  $b_3 = 2 + 2h_{2,1}$ , two independent ‘bulk’ 3-cycles are inherited from the six-torus and ten additional exceptional 3-cycles arise at the  $\mathbb{Z}_2$  fix-points.

### 2.1 Bulk 3-cycles

Any basic factorizable 3-cycle on  $\prod_{k=1}^3 T_k^2$  can be represented in terms of the basic 1-cycles of each 2-torus,  $\pi_{2k-1}$  and  $\pi_{2k}$ , as a direct product  $\pi_{i,j,m} = \pi_i \otimes \pi_j \otimes \pi_m$ . Out of the  $2^3$  different

<sup>2</sup>There exists a second, inequivalent possibility with  $\mathbb{Z}_6$  symmetry, having the shift vector  $v = (1/6, 1/3, -1/2)$ , which is often denoted as  $\mathbb{Z}'_6$ . Both symmetric orbifolds in the IIA picture are T-dual to asymmetric orbifolds in the IIB background. Our models are therefore not T-dual to the symmetric  $\mathbb{Z}_6$  orbifold of IIB in [67].

<sup>3</sup>The volume is not zero in the stringy sense, i.e. a non-vanishing string tension is generated by a discrete NS-NS two-form background in the ten dimensional language. For more details see e.g. the review article [68].

combinations, one can construct only two linearly independent bulk cycles which are invariant under the orbifold action. A convenient choice for them is given by

$$\begin{aligned}\rho_1 &= 2[(1+\theta+\theta^2)\pi_{1,3,5}] = 2(\pi_{1,3,5} + \pi_{2,4,-6} + \pi_{2-1,4-3,6-5}) \\ &= 2(\pi_{1,4,5} + \pi_{1,3,6} + \pi_{2,3,5} - \pi_{1,4,6} - \pi_{2,4,5} - \pi_{2,3,6}), \\ \rho_2 &= 2[(1+\theta+\theta^2)\pi_{2,3,5}] = 2(\pi_{2,3,5} + \pi_{2-1,4,-6} + \pi_{-1,4-3,6-5}) \\ &= 2(\pi_{1,4,5} + \pi_{1,3,6} + \pi_{2,3,5} - \pi_{1,3,5} - \pi_{2,4,6}).\end{aligned}\quad (3)$$

The factor of two in (3) arises due to the trivial action of  $\theta^3$  on any 3-cycle. Any orbifold invariant non-factorizable 3-cycle can be written as a linear combination of these two bulk cycles.

The coefficients of the factorizable 3-cycles are determined by the wrapping numbers  $n_k$  and  $m_k$  along the basic 1-cycles  $\pi_{2k-1}$  and  $\pi_{2k}$  on the 2-torus  $T_k^2$  and their orbifold images,

$$\begin{pmatrix} n_1 & m_1 \\ n_2 & m_2 \\ n_3 & m_3 \end{pmatrix} \xrightarrow{\theta} \begin{pmatrix} -m_1 & n_1 + m_1 \\ -m_2 & n_2 + m_2 \\ m_3 & -(n_3 + m_3) \end{pmatrix} \xrightarrow{\theta} \begin{pmatrix} -(n_1 + m_1) & n_1 \\ -(n_2 + m_2) & n_2 \\ -(n_3 + m_3) & n_3 \end{pmatrix}. \quad (4)$$

Starting with the 3-cycle  $(n_1^a\pi_1 + m_1^a\pi_2) \otimes (n_2^a\pi_3 + m_2^a\pi_4) \otimes (n_3^a\pi_5 + m_3^a\pi_6)$  and adding its orbifold images, the invariant bulk 3-cycle is of the form

$$\Pi_a = Y_a\rho_1 + Z_a\rho_2, \quad (5)$$

where the coefficients  $Y_a$  and  $Z_a$  are given by linear combinations of products of the elementary wrapping numbers,

$$\begin{aligned}Y_a &\equiv n_1^a n_2^a n_3^a - \sum_{i \neq j \neq k \neq i} m_i^a m_j^a n_k^a - m_1^a m_2^a m_3^a, \\ Z_a &\equiv \sum_{i \neq j \neq k \neq i} m_i^a m_j^a n_k^a + \sum_{i \neq j \neq k \neq i} m_i^a n_j^a n_k^a.\end{aligned}\quad (6)$$

In computing the intersection numbers of the two independent bulk cycles which are invariant under an  $\mathbb{Z}_N$  action, the orbifold projection has to be taken into account,

$$\Pi_a \circ \Pi_b = \frac{1}{N} \left( \sum_{i=1}^{N-1} \theta^i \pi_a \right) \circ \left( \sum_{j=1}^{N-1} \theta^j \pi_b \right). \quad (7)$$

This leads to the intersection numbers of the two fundamental bulk cycles (3),

$$\rho_1 \circ \rho_2 = -2, \quad \rho_1 \circ \rho_1 = \rho_2 \circ \rho_2 = 0, \quad (8)$$

and for general bulk cycles  $\Pi_a = Y_a\rho_1 + Z_a\rho_2$ , we always obtain even intersection numbers,

$$I_{ab} \equiv \Pi_a \circ \Pi_b = 2(Z_a Y_b - Y_a Z_b). \quad (9)$$

## 2.2 Exceptional 3-cycles

Exceptional 3-cycles in the orbifold limit only occur in the  $\theta^3$  sector. They consist of products of 2-cycles which are stuck at the  $\mathbb{Z}_2$  fixed points and have zero volume in the orbifold limit on  $T_1^2 \times T_2^2$  times a 1-cycle on  $T_3^2$ . The fixed point 1 in the origin of each 2-torus is already

invariant under the orbifold generator  $\theta$ . The other three  $\mathbb{Z}_2$  fixed points are permuted by the  $\mathbb{Z}_6$  symmetry in the following way,

$$\theta(4) = 5, \quad \theta(5) = 6, \quad \theta(6) = 4. \quad (10)$$

Similarly, every 1-cycle on  $T_3^2$  is invariant under  $\theta^3$ , but the  $\mathbb{Z}_6$  generator acts as follows,

$$\theta(\pi_5) = -\pi_6, \quad \theta(\pi_6) = \pi_{5-6} = \pi_5 - \pi_6. \quad (11)$$

Thus, the exceptional 3-cycles are given by orbifold invariant combinations of the products of 2- and 1-cycles,

$$(1 + \theta + \theta^2)(e_{ij} \otimes \pi_k) \quad \text{with} \quad i, j = 1, 4, 5, 6; \quad k = 5, 6, \quad (12)$$

where the orbifold images are given by  $\theta(e_{ij} \otimes \pi_k) = e_{\theta(i)\theta(j)} \otimes \theta(\pi_k)$ . This ansatz leads to ten linearly independent exceptional cycles,

$$\begin{aligned} \varepsilon_1 &= (e_{41} - e_{61}) \otimes \pi_5 + (e_{61} - e_{51}) \otimes \pi_6, & \tilde{\varepsilon}_1 &= (e_{51} - e_{61}) \otimes \pi_5 + (e_{41} - e_{51}) \otimes \pi_6, \\ \varepsilon_2 &= (e_{14} - e_{16}) \otimes \pi_5 + (e_{16} - e_{15}) \otimes \pi_6, & \tilde{\varepsilon}_2 &= (e_{15} - e_{16}) \otimes \pi_5 + (e_{14} - e_{15}) \otimes \pi_6, \\ \varepsilon_3 &= (e_{44} - e_{66}) \otimes \pi_5 + (e_{66} - e_{55}) \otimes \pi_6, & \tilde{\varepsilon}_3 &= (e_{55} - e_{66}) \otimes \pi_5 + (e_{44} - e_{55}) \otimes \pi_6, \\ \varepsilon_4 &= (e_{45} - e_{64}) \otimes \pi_5 + (e_{64} - e_{56}) \otimes \pi_6, & \tilde{\varepsilon}_4 &= (e_{56} - e_{64}) \otimes \pi_5 + (e_{45} - e_{56}) \otimes \pi_6, \\ \varepsilon_5 &= (e_{46} - e_{65}) \otimes \pi_5 + (e_{65} - e_{54}) \otimes \pi_6, & \tilde{\varepsilon}_5 &= (e_{54} - e_{65}) \otimes \pi_5 + (e_{46} - e_{54}) \otimes \pi_6. \end{aligned} \quad (13)$$

This construction resembles very much the one in [36]. The intersection numbers of exceptional cycles are computed from the self intersection number  $-2$  of any exceptional cycle  $e_{ij}$  stuck at a  $\mathbb{Z}_2$  singularity and the intersection numbers of the 1-cycles on  $T_3^2$ , taking into account the factors from the orbifold projection similarly to equation (7). The result

$$\varepsilon_i \circ \tilde{\varepsilon}_j = -2\delta_{ij}, \quad \varepsilon_i \circ \varepsilon_j = \tilde{\varepsilon}_i \circ \tilde{\varepsilon}_j = 0, \quad (14)$$

leads to the intersection matrix for exceptional cycles

$$I_\varepsilon = \bigoplus_{j=1}^5 \begin{pmatrix} 0 & -2 \\ 2 & 0 \end{pmatrix}. \quad (15)$$

### 2.3 An integral basis

The intersection numbers of pure bulk cycles (8) and pure exceptional cycles (15) are always even. It is therefore possible to construct fractional cycles of the form  $\frac{1}{2}\Pi^{bulk} + \frac{1}{2}\Pi^{exceptional}$  which form an unimodular lattice as required by Poincaré duality [71].

For example, a D6-brane with wrapping numbers  $(n_1, m_1; n_2, m_2; n_3, m_3) = (1, 0; 1, 0; 1, 0)$  and its orbifold images wrap the bulk cycle  $\rho_1$  and pass through the fixed points  $e_{kl}$  with  $k, l \in \{1, 4\}$  as well as their orbifold images. The orbits of the three non-trivial fixed points  $e_{14}, e_{41}, e_{44}$  generate the exceptional cycles  $\varepsilon_1, \varepsilon_2$  and  $\varepsilon_3$  while the orbit of  $e_{11}$  vanishes. In this case, a valid fractional cycle is given by

$$\frac{1}{2}\rho_1 \pm \frac{1}{2}(\varepsilon_1 \pm \varepsilon_2 \pm \varepsilon_3) \quad (16)$$

with arbitrary relative signs for the exceptional contributions.

This argument can be repeated for different wrapping numbers and 3-cycles which do not pass through  $e_{11}$  but instead are displaced by  $\sum_{i=1}^4 \sigma_i \pi_i$  (with  $\sigma_i \in \{0, \frac{1}{2}\}$ ) from the origins of  $T_1^2$  and  $T_2^2$ . All possible combinations of wrapping numbers of the bulk 3-cycles with fixed points are listed in table 23. From this, we can obtain a basis for the unimodular lattice of 3-cycles

$$\begin{aligned}
\alpha_1 &= \frac{1}{2}\rho_1 + \frac{1}{2}(\varepsilon_1 + \varepsilon_2 + \varepsilon_3), & \alpha_5 &= \frac{1}{2}(\varepsilon_1 - \varepsilon_3 + \varepsilon_4 + \varepsilon_5), \\
\alpha_2 &= \frac{1}{2}\rho_2 - \frac{1}{2}(\tilde{\varepsilon}_1 + \tilde{\varepsilon}_2 + \tilde{\varepsilon}_3), & \alpha_6 &= \frac{1}{2}(-\tilde{\varepsilon}_1 + \tilde{\varepsilon}_3 + \tilde{\varepsilon}_4 - \tilde{\varepsilon}_5), \\
\alpha_3 &= \frac{1}{2}\rho_1 + \frac{1}{2}(\varepsilon_1 - \varepsilon_2 + \varepsilon_3), & \alpha_7 &= \frac{1}{2}(\tilde{\varepsilon}_1 - \tilde{\varepsilon}_3 - \tilde{\varepsilon}_4 - \tilde{\varepsilon}_5), \\
\alpha_4 &= \frac{1}{2}\rho_2 - \frac{1}{2}(\tilde{\varepsilon}_1 - \tilde{\varepsilon}_2 + \tilde{\varepsilon}_3), & \alpha_8 &= \frac{1}{2}(\varepsilon_1 - \varepsilon_3 + \varepsilon_4 - \varepsilon_5), \\
\alpha_9 &= -\frac{1}{2}\rho_1 + \frac{1}{2}(-\varepsilon_3 + \varepsilon_4 - \tilde{\varepsilon}_1 + \tilde{\varepsilon}_3 + 2\tilde{\varepsilon}_4), & & \\
\alpha_{10} &= \frac{1}{2}\rho_2 + \frac{1}{2}(\varepsilon_1 - \varepsilon_3 + 2\varepsilon_4 - \tilde{\varepsilon}_1 + \tilde{\varepsilon}_4), & & \\
\alpha_{11} &= \frac{1}{2}(\rho_1 - \rho_2) + (\varepsilon_1 + \varepsilon_4 + \tilde{\varepsilon}_3 + \tilde{\varepsilon}_4), & & \\
\alpha_{12} &= \frac{1}{2}(-\rho_1 - 2\rho_2) + (-\varepsilon_3 + \varepsilon_4 + \tilde{\varepsilon}_1 + \tilde{\varepsilon}_3), & &
\end{aligned} \tag{17}$$

with an intersection matrix

$$I_{\mathbb{Z}_6} = \text{diag} \left( \left( \begin{array}{cc} 0 & 1 \\ -1 & 0 \end{array} \right), \dots, \left( \begin{array}{cc} 0 & 1 \\ -1 & 0 \end{array} \right) \right). \tag{18}$$

## 2.4 Orientifold projection

The aim of this work is to find stable and supersymmetric models. In order to cancel the RR charge of the D6-branes, orientifold 6-planes are required. Such O6-planes arise naturally, if the worldsheet parity  $\Omega$  is chosen to be accompanied by an antiholomorphic involution  $\mathcal{R}$ , which we can choose to be the complex conjugation

$$\mathcal{R} : \quad z^k \rightarrow \bar{z}^k \quad \text{for } k = 1, 2, 3, \tag{19}$$

where  $z^k = x^{2+2k} + ix^{3+2k}$  are the complex coordinates on every 2-torus  $T_k^2$ .

### 2.4.1 Orientifold images of bulk cycles

In order to be consistent with the compactification,  $\mathcal{R}$  has to be an automorphism of the  $\mathbb{Z}_6$  invariant lattice. This leads to two possible orientations **A** and **B** of each 2-torus with a lattice basis and its dual which are given explicitly in appendix A. In terms of the notation of figure 1, the different orientations lead to the following projections of the fundamental 1-cycles under  $\mathcal{R}$ ,

$$\mathbf{A} : \left\{ \begin{array}{l} \pi_{2k-1} \xrightarrow{\mathcal{R}} \pi_{2k-1}, \\ \pi_{2k} \xrightarrow{\mathcal{R}} \pi_{2k-1} - \pi_{2k}, \end{array} \right. \quad \mathbf{B} : \pi_{2k-1} \xleftrightarrow{\mathcal{R}} \pi_{2k}. \tag{20}$$

The geometry of the first two 2-tori is identical because the orbifold generator acts in the same way. Consequently, only six of the  $2^3$  naive choices are inequivalent while the choices **AB** and

| $\mathcal{R}$ images of bulk cycles |                        |                        |
|-------------------------------------|------------------------|------------------------|
| lattice                             | $\mathcal{R} : \rho_1$ | $\mathcal{R} : \rho_2$ |
| <b>AAA</b>                          | $\rho_1$               | $\rho_1 - \rho_2$      |
| <b>AAB</b>                          | $\rho_2$               | $\rho_1$               |
| <b>ABA</b>                          | $\rho_2$               | $\rho_1$               |
| <b>ABB</b>                          | $\rho_2 - \rho_1$      | $\rho_2$               |
| <b>BBA</b>                          | $\rho_2 - \rho_1$      | $\rho_2$               |
| <b>BBB</b>                          | $-\rho_1$              | $\rho_2 - \rho_1$      |

Table 1:  $\mathcal{R}$  images of cycles inherited from the torus in the orbifold limit  $T^6/(\mathbb{Z}_6 \times \Omega\mathcal{R})$ .

**BA** for  $T_1^2 \times T_2^2$  lead to identical results. Evaluating the projection (20) on the right hand side of (3) leads to the orientifold images of bulk cycles displayed in table 1.

The bulk cycles which are invariant under  $\mathcal{R}$  are easily read off from table 1. However, in order to determine the homology classes of the O6-planes, the factorizable 3-cycles have to be considered in more detail. The O6-planes can be decomposed into two orbits which are invariant under  $\Omega\mathcal{R}\theta^{2k}$  and  $\Omega\mathcal{R}\theta^{2k+1}$ . The corresponding wrapping numbers, the coefficients  $Y$  and  $Z$  of the homological cycles (see eq. (6)), and bulk cycles are listed in table 2. The over-all cycle which is wrapped by the orientifold plane is given by the sum of the two orbits.

#### 2.4.2 Orientifold images of exceptional cycles

In order to find the correct transformations under the orientifold projection, the transformations of the relevant fixed points on  $T_1^2 \times T_2^2$  under  $\mathcal{R}$  have to be taken into account,

$$\mathbf{A} : \begin{cases} 1 \xrightarrow{\mathcal{R}} 1, \\ 4 \xrightarrow{\mathcal{R}} 4, \\ 5 \xleftarrow{\mathcal{R}} 6, \end{cases} \quad \mathbf{B} : \begin{cases} 1 \xrightarrow{\mathcal{R}} 1, \\ 4 \xleftarrow{\mathcal{R}} 5, \\ 6 \xrightarrow{\mathcal{R}} 6, \end{cases} \quad (21)$$

and the 1-cycle on  $T_3^2$  transforms according to (20).

The images under the reflection  $\mathcal{R}$  for all inequivalent lattices are displayed in table 3.

#### 2.4.3 RR tadpole cancellation

The most important consistency requirement on the cohomology classes of the forms which live on the world volume of the D6-branes is that the charge of the RR 7-form which couples to the D6-branes and O6-planes vanishes. The Poincaré duals of these 7-forms are homology classes (see e.g. [9]), implying that the RR tadpole cancellation conditions can be reformulated in terms of the bulk and exceptional 3-cycles discussed above.

The O6-planes only wrap bulk 3-cycles whereas D6-branes can wrap both exceptional and

| O6-planes for $T^6/(\mathbb{Z}_6 \times \Omega\mathcal{R})$ |                                  |     |     |                        |
|---|----------------------------------|-----|-----|------------------------|
| lattice   | $(n_1, m_1; n_2, m_2; n_3, m_3)$ | $Y$ | $Z$ | cycle                  |
| <b>AAA</b>  | (1, 0; 1, 0; 1, 0)               | 1   | 0   | $\rho_1$               |
|   | (1, 1; 1, 1; 1, -1)              | 3   | 0   | $3\rho_1$              |
| <b>AAB</b>  | (1, 0; 1, 0; 1, 1)               | 1   | 1   | $\rho_1 + \rho_2$      |
|   | (1, 1; 1, 1; 2, -1)              | 3   | 3   | $3(\rho_1 + \rho_2)$   |
| <b>ABA</b>  | (1, 0; 1, 1; 1, 0)               | 1   | 1   | $\rho_1 + \rho_2$      |
|   | (1, 1; 0, 1; 1, -1)              | 1   | 1   | $\rho_1 + \rho_2$      |
| <b>ABB</b>  | (1, 0; 1, 1; 1, 1)               | 0   | 3   | $3\rho_2$              |
|   | (1, 1; 0, 1; 2, -1)              | 0   | 3   | $3\rho_2$              |
| <b>BBA</b>  | (1, 1; 1, 1; 1, 0)               | 0   | 3   | $3\rho_2$              |
|   | (0, 1; 0, 1; 1, -1)              | 0   | 1   | $\rho_2$               |
| <b>BBB</b>  | (1, 1; 1, 1; 1, 1)               | -3  | 6   | $3(-\rho_1 + 2\rho_2)$ |
|   | (0, 1; 0, 1; 2, -1)              | -1  | 2   | $-\rho_1 + 2\rho_2$    |

Table 2: O6-planes for  $T^6/(\mathbb{Z}_6 \times \Omega\mathcal{R})$ . In each case, the wrapping numbers of an arbitrary element of a  $\mathbb{Z}_6$  orbit are listed. The coefficients  $Y, Z$  are computed from (6). The total homology class of the O6-planes is given by the sum over the two orbits for each lattice.

bulk 3-cycles. The general condition of an over-all vanishing homology class is given by

$$\sum_a N_a (\Pi_a + \Pi_{a'}) - 4\Pi_{O6} = 0, \quad (22)$$

and can be evaluated in detail using tables 1 and 3 where by  $\Pi_{a'}$  we denote the  $\mathcal{R}$  image of the 3-cycle  $\Pi_a$ . For the six inequivalent lattice orientations and only bulk branes we obtain

$$\begin{aligned}
& \mathbf{AAA} : \sum_a N_a (2Y_a + Z_a) \rho_1 = 2^4 \rho_1, \\
& \mathbf{AAB} : \sum_a N_a (Y_a + Z_a) (\rho_1 + \rho_2) = 2^4 (\rho_1 + \rho_2), \\
& \mathbf{ABA} : \sum_a N_a (Y_a + Z_a) (\rho_1 + \rho_2) = 2^3 (\rho_1 + \rho_2), \\
& \mathbf{ABB} : \sum_a N_a (Y_a + 2Z_a) \rho_2 = 3 \cdot 2^3 \rho_2, \\
& \mathbf{BBA} : \sum_a N_a (Y_a + 2Z_a) \rho_2 = 2^4 \rho_2, \\
& \mathbf{BBB} : \sum_a N_a Z_a (-\rho_1 + 2\rho_2) = 2^4 (-\rho_1 + 2\rho_2).
\end{aligned} \quad (23)$$

Here,  $N_a$  is the number of D6-branes wrapping the cycle  $\Pi_a$ , the so-called stacksize. These

| $\mathcal{R}$ images of exceptional cycles for $T^6/(\mathbb{Z}_6 \times \Omega\mathcal{R})$ |   |   |   |   |   |   |   |   |   |   |
|--|---|---|---|---|---|---|---|---|---|---|
| lattice  | $\mathcal{R} : \varepsilon_1$           | $\mathcal{R} : \varepsilon_2$           | $\mathcal{R} : \varepsilon_3$           | $\mathcal{R} : \varepsilon_4$           | $\mathcal{R} : \varepsilon_5$           | $\mathcal{R} : \tilde{\varepsilon}_1$   | $\mathcal{R} : \tilde{\varepsilon}_2$   | $\mathcal{R} : \tilde{\varepsilon}_3$   | $\mathcal{R} : \tilde{\varepsilon}_4$   | $\mathcal{R} : \tilde{\varepsilon}_5$   |
| <b>AAA</b>   | $\varepsilon_1$                         | $\varepsilon_2$                         | $\varepsilon_3$                         | $\varepsilon_5$                         | $\varepsilon_4$                         | $\varepsilon_1 - \tilde{\varepsilon}_1$ | $\varepsilon_2 - \tilde{\varepsilon}_2$ | $\varepsilon_3 - \tilde{\varepsilon}_3$ | $\varepsilon_5 - \tilde{\varepsilon}_5$ | $\varepsilon_4 - \tilde{\varepsilon}_4$ |
| <b>AAB</b>   | $\tilde{\varepsilon}_1$                 | $\tilde{\varepsilon}_2$                 | $\tilde{\varepsilon}_3$                 | $\tilde{\varepsilon}_5$                 | $\tilde{\varepsilon}_4$                 | $\varepsilon_1$                         | $\varepsilon_2$                         | $\varepsilon_3$                         | $\varepsilon_5$                         | $\varepsilon_4$                         |
| <b>ABA</b>   | $\varepsilon_1$                         | $\tilde{\varepsilon}_2 - \varepsilon_2$ | $\varepsilon_4$                         | $\varepsilon_3$                         | $\varepsilon_5$                         | $\varepsilon_1 - \tilde{\varepsilon}_1$ | $\tilde{\varepsilon}_2$                 | $\varepsilon_4 - \tilde{\varepsilon}_4$ | $\varepsilon_3 - \tilde{\varepsilon}_3$ | $\varepsilon_5 - \tilde{\varepsilon}_5$ |
| <b>ABB</b>   | $\tilde{\varepsilon}_1$                 | $-\varepsilon_2$                        | $\tilde{\varepsilon}_4$                 | $\tilde{\varepsilon}_3$                 | $\tilde{\varepsilon}_5$                 | $\varepsilon_1$                         | $\tilde{\varepsilon}_2 - \varepsilon_2$ | $\varepsilon_4$                         | $\varepsilon_3$                         | $\varepsilon_5$                         |
| <b>BBA</b>   | $\tilde{\varepsilon}_1 - \varepsilon_1$ | $\tilde{\varepsilon}_2 - \varepsilon_2$ | $\tilde{\varepsilon}_3 - \varepsilon_3$ | $\tilde{\varepsilon}_5 - \varepsilon_5$ | $\tilde{\varepsilon}_4 - \varepsilon_4$ | $\tilde{\varepsilon}_1$                 | $\tilde{\varepsilon}_2$                 | $\tilde{\varepsilon}_3$                 | $\tilde{\varepsilon}_5$                 | $\tilde{\varepsilon}_4$                 |
| <b>BBB</b>   | $-\varepsilon_1$                        | $-\varepsilon_2$                        | $-\varepsilon_3$                        | $-\varepsilon_5$                        | $-\varepsilon_4$                        | $\tilde{\varepsilon}_1 - \varepsilon_1$ | $\tilde{\varepsilon}_2 - \varepsilon_2$ | $\tilde{\varepsilon}_3 - \varepsilon_3$ | $\tilde{\varepsilon}_5 - \varepsilon_5$ | $\tilde{\varepsilon}_4 - \varepsilon_4$ |

Table 3:  $\mathcal{R}$  images of the exceptional cycles for  $T^6/(\mathbb{Z}_6 \times \Omega\mathcal{R})$ .

conditions are easily generalized for fractional D6-branes with a bulk part  $\frac{1}{2}(Y_a\rho_1 + Z_a\rho_2)$  by inserting the corresponding factor  $1/2$  on the left hand side of (23).

For exceptional cycles, the over-all homology class has to cancel among all D6-branes and their  $\mathcal{R}$ -images by themselves, because the O6-plane does not contribute.

The same results can be obtained by computing the loop channel annulus, Möbius strip and Klein bottle amplitude and performing the modular transformation to the RR-tree channel. For more details on the open string amplitudes and massless spectrum see section 3.

## 2.5 Supersymmetry conditions

### 2.5.1 Supersymmetric bulk cycles

Factorizable 3-cycles preserve  $\mathcal{N} = 1$  supersymmetry provided that the sum over the three angles w.r.t. the  $\mathcal{R}$  invariant plane on all 2-tori vanishes. It is convenient to reformulate the supersymmetry condition in terms of the coefficients  $Y, Z$  (see eq. (6)) as follows. If  $\pi\varphi_a^k$  is the angle w.r.t.  $\pi_{2k-1}$  of the bulk cycle  $\Pi_a$  represented by the wrapping numbers  $(n_k^a, m_k^a)$ , we have

$$\tan(\pi\varphi_a^k) = \sqrt{3} \frac{m_k^a}{2n_k^a + m_k^a}. \quad (24)$$

On an **A** lattice,  $\pi\varphi_a^k$  is also the angle w.r.t. the  $\mathcal{R}$  invariant axis, whereas on a **B** lattice it is given by  $\pi\varphi_a^k - \frac{\pi}{6}$ . We can combine both possibilities in the single equation  $\pi\tilde{\varphi}_a^k = \pi(\varphi_a^k - \frac{b_k}{6})$ , where  $b_k = 0$  for an **A** and  $b_k = 1$  for a **B** torus. The necessary condition for a supersymmetric factorizable bulk cycle is given in terms of the tangents by  $\sum_{k=1}^3 \tan(\pi\tilde{\varphi}_a^k) = \prod_{k=1}^3 \tan(\pi\tilde{\varphi}_a^k)$ . Evaluating this equation for the six inequivalent choices of lattice orientations and using (24), we obtain

$$\begin{aligned} \mathbf{AAA} : & Z_a = 0, \\ \mathbf{AAB} : & Y_a - Z_a = 0, \\ \mathbf{ABA} : & Y_a - Z_a = 0, \\ \mathbf{ABB} : & Y_a = 0, \\ \mathbf{BBA} : & Y_a = 0, \\ \mathbf{BBB} : & 2Y_a + Z_a = 0. \end{aligned} \quad (25)$$

By the analysis of the angle criterion, we recover the result obtained by stating that the supersymmetric cycles are those special Lagrangian cycles which are calibrated w.r.t. the same holomorphic 3-form as the ones wrapped by the O6-planes. Stated differently, the vanishing coefficients in (25) are also those which are zero in table 2. Therefore up to normalization the supersymmetric D6-branes wrap the same bulk 3-cycle as the O6-planes, and by this the intersection between the two always vanishes,

$$\Pi_a \circ \Pi_{O6} = 0. \quad (26)$$

There remains a little subtlety: since the tangent is periodic in  $\pi$ , the condition above does not distinguish between D6-branes and anti-D6-branes. However, a D6-brane gives a positive contribution to the untwisted RR charge on the left hand side of (23). The sufficient second condition for a supersymmetric bulk 3-cycle therefore reads

$$\mathbf{AAA}, \mathbf{AAB}, \mathbf{ABA} : Y_a > 0, \quad \mathbf{ABB}, \mathbf{BBA}, \mathbf{BBB} : Z_a > 0. \quad (27)$$

### 2.5.2 Supersymmetry condition on exceptional cycles

Fractional branes preserve supersymmetry provided that their contribution from the exceptional cycles arises only from fixed points on the first two 2-tori which are traversed by the supersymmetric bulk part of the 2-cycle times a 1-cycle on  $T_3^2$ . All possible combinations of factorizable 2-cycles on  $T_1^2 \times T_2^2$  and  $\mathbb{Z}_2$  fixed points which they traverse are displayed in table 23. The corresponding exceptional cycles can be read off from table 24.

In all cases where the bulk part of the cycle passes through the origin of  $T_1^2 \times T_2^2$ , the signs of the contributions from the three non-trivial fixed points are arbitrary. However, if the bulk cycle does not pass through the origin, exceptional cycles arise from four non-trivial fixed points. In this case, three signs can be chosen independently while the fourth one is determined to be the product of the other three. This is due to the fact that relative Wilson lines  $\frac{\tau_k}{2} \in \{0, 1/2\}$  between two branes are associated to the  $\mathbb{Z}_2$  fixed points on  $T_k^2$ . Since in our convention, the fixed points are localized on  $T_1^2 \times T_2^2$ , discrete Wilson lines naturally occur on these two tori (compare also with [67]). We choose the convention such that for vanishing Wilson lines all fixed points contribute with the same sign. The relative signs between exceptional 2-cycles are then given as follows,

$$\tau_0 (e_{ik} + (-1)^{\tau_1} e_{jk} + (-1)^{\tau_2} e_{il} + (-1)^{\tau_1 + \tau_2} e_{jl}) = \tau_0 e_{ik} + \tau'_1 e_{jk} + \tau'_2 e_{il} + \tau_0 \tau'_1 \tau'_2 e_{jl}, \quad (28)$$

where  $\tau_0 = \pm 1$  is the global sign of contributions from exceptional cycles corresponding to the two possible  $\mathbb{Z}_2$  eigenvalues and  $\tau'_k = \tau_0 (-1)^{\tau_k}$  for  $k = 1, 2$ . The allowed relative signs for combinations of exceptional 3-cycles associated to a specific bulk cycle are obtained by means of table 24.

## 3 Massless open string spectrum: tree and loop amplitudes

A stack of  $N_a$  identical fractional D6-branes in general supports the gauge group  $U(N_a)$  and preserves  $\mathcal{N} = 2$  supersymmetry by itself. This is in contrast to the compactifications on  $T^6$  [5, 6, 20],  $T^6/\mathbb{Z}_3$  [23],  $T^6/(\mathbb{Z}_3 \times \mathbb{Z}_3)$ ,  $T^6/(\mathbb{Z}_2 \times \mathbb{Z}_2)$  [28] and  $T^6/(\mathbb{Z}_4 \times \mathbb{Z}_2)$  [37] which admit only pure bulk 3-cycles and hence preserve  $\mathcal{N} = 4$  supersymmetry in the gauge sector. However,

also on  $T^6/\mathbb{Z}_6$ , additional chiral multiplets in the adjoint representation arise at intersections of branes with their orbifold images as explained below.

The chiral part of the open string spectrum can be directly derived from the intersections of the 3-cycles in a given configuration as displayed in table 4, whereas the knowledge of the non-

| multiplicity  | rep.                                      |
|---|---|
| $\Pi_a \circ \Pi_b$   | $(\mathbf{N}_a, \overline{\mathbf{N}}_b)$ |
| $\Pi_a \circ \Pi_{b'}$                                      | $(\mathbf{N}_a, \mathbf{N}_b)$            |
| $\frac{1}{2} (\Pi_a \circ \Pi_{a'} - \Pi_a \circ \Pi_{O6})$ | <b>Sym</b> <sub><i>a</i></sub>            |
| $\frac{1}{2} (\Pi_a \circ \Pi_{a'} + \Pi_a \circ \Pi_{O6})$ | <b>Anti</b> <sub><i>a</i></sub>           |

Table 4: Generic chiral spectrum of intersecting D6-branes.

chiral states such as Higgs particles in a standard model compactification or multiplets in the adjoint representation requires a detailed analysis of the string amplitudes or the computation of the Chan-Paton label for each massless open string state. Both techniques are briefly discussed in this section in order to show manifestly that our choice of Chan-Paton matrices and the sign of the orientifold projection on the exceptional cycles are appropriate. Furthermore, by using both techniques simultaneously, ambiguities in relative signs can be eliminated.

### 3.1 Boundary states for fractional intersecting branes

The untwisted and twisted boundary states are directly related to the bulk and exceptional cycles wrapped by fractional D6-branes. After applying a modular transformation on the scattering amplitudes between two D6-branes and between an O6-plane and a D6-brane, one obtains the two open string 1-loop amplitudes, the annulus and the Möbius strip. From these two, we can read off the complete massless spectrum.

The boundary state of an arbitrary fractional D6-brane consists of an untwisted part  $|U_a\rangle$ , corresponding to the wrapped bulk cycle  $\Pi_a^{bulk}$ , and a twisted part  $|T_a\rangle$ , coming from the exceptional cycles  $\Pi_a^{ex}$  stuck at the traversed  $\mathbb{Z}_2$  fixed points,

$$|B_a\rangle = |U_a\rangle + |T_a\rangle. \quad (29)$$

For a pure bulk D6-brane, the complete boundary state is given by

$$|U_a\rangle = c_U \left( \prod_{k=1}^3 L_k^a \right) \left( \sum_{l=0}^2 |D6; \theta^l(n_i^a, m_i^a)\rangle \right), \quad (30)$$

where in  $c_U$  all universal factors of the normalization have been absorbed.

$L_k^a = \sqrt{(n_k^a)^2 + n_k^a m_k^a + (m_k^a)^2}$  is the length of the 1-cycle wrapping  $T_k^2$  measured in units of its radius  $R_k$ , and  $\theta^l(n_i^a, m_i^a)$  labels a factorizable 3-cycle with wrapping numbers  $(n_i^a, m_i^a)$  ( $i = 1, 2, 3$ ) and its orbifold images.

A fractional brane wraps only  $\frac{1}{2}\Pi_a^{bulk}$ . Accordingly, the normalization constant of the untwisted boundary state changes,  $c_U \rightarrow c_U/2$ , and the twisted parts of the boundary states are

of the form

$$|T_a\rangle = c_T L_3^a \sum_{i,j} \alpha_{ij} \left( \sum_{l=0}^2 |D6; \theta^l(n_3^a, m_3^a), \theta^l(e_{ij})\rangle \right) \quad (31)$$

where all universal factors of the normalization have been absorbed in  $c_T$ . The relative factor  $c_T/c_U$  is fixed by worldsheet duality. The twisted boundary states depend only on the wrapping numbers on  $T_3^2$  and are stuck at those  $\mathbb{Z}_2$  fixed points  $e_{ij}$  ( $i, j = 1, 4, 5, 6$ ) on  $T_1^2 \times T_2^2$  which are traversed by the bulk cycle. The relative signs  $\alpha_{ij} = \pm 1$  for different fixed points correspond to the  $\mathbb{Z}_2$  eigenvalue and discrete Wilson lines displayed in equation (28).

The oscillator expansion of the boundary states and zero mode contributions in the annulus amplitude including discrete Wilson lines are stated in appendix C.

The untwisted crosscap states are constructed in a similar way to the boundary states. Since the total homology class of the O6-planes is composed of two independent orbits as shown in table 2, the crosscap state contains two kinds of contributions,

$$|C\rangle = \mathcal{N}_{even} \left( \sum_{k=0}^2 |\Omega\mathcal{R}\theta^{2k}\rangle \right) + \mathcal{N}_{odd} \left( \sum_{k=0}^2 |\Omega\mathcal{R}\theta^{2k+1}\rangle \right), \quad (32)$$

where the normalizations  $\mathcal{N}_{even}$ ,  $\mathcal{N}_{odd}$  depend on the choice of the lattice orientation and can be deduced from worldsheet duality using the explicit calculation in [4]. In particular, for an **AB** lattice on  $T_1^2 \times T_2^2$  they are identical.

From (30), (31) and (32), the tree channel amplitudes can be computed and then transformed to the loop channel.

### 3.2 Loop channel amplitudes

The open string 1-loop amplitudes are given by

$$\mathcal{A} + \mathcal{M} = c \int_0^\infty \frac{dt}{t^3} \text{Tr}_{open} (\mathbf{P}_{orb} \mathbf{P}_{GSO} \mathbf{P}_{\Omega\mathcal{R}} (-1)^{\mathbf{S}} e^{-2\pi t L_0}) \quad (33)$$

with the projectors  $\mathbf{P}_{orb} = \frac{1}{6} \sum_{k=0}^5 \theta^k$ ,  $\mathbf{P}_{GSO} = \frac{1}{2}(1 + (-1)^F)$  and  $\mathbf{P}_{\Omega\mathcal{R}} = \frac{1}{2}(1 + \Omega\mathcal{R})$  and  $\text{Tr}_{open}$  running over the NS and R sector weighted by  $(-1)^{\mathbf{S}}$  where  $\mathbf{S}$  is the space-time fermion number. The massless spectrum can be read off from (33) by a power series expansion.

In the following, we restrict to supersymmetric configurations and compute only the number of fermionic degrees of freedom.

#### 3.2.1 Adjoint and bifundamental representations: Annulus

A general element of the orbifold group exchanges D6-branes with their images. Only a  $\mathbb{Z}_2$  twist preserves the brane configuration, such that the only non-vanishing contributions to the annulus amplitude for bulk branes are given by

$$\mathcal{A} = \frac{c}{24} \int_0^\infty \frac{dt}{t^3} \text{Tr}_{open} ((1 + \theta^3)(1 + (-1)^F)(-1)^{\mathbf{S}} e^{-2\pi t L_0}). \quad (34)$$

The generic form of lattice contributions to the amplitudes per 2-torus is displayed in (62) and the oscillator contributions are listed in (65).

Since the R sector with  $(-1)^F$  insertion always has a vanishing contribution to the loop channel amplitudes, the massless fermionic spectrum for bulk D6-branes at generic angles  $\varphi_k^{ab}$  is computed from

$$\mathcal{A}_R = \sum_{a,b} \frac{c}{24} \int_0^\infty \frac{dt}{t^3} \left( (2N_a)(2N_b) I_{ab} \mathcal{A}_{0,(\varphi_1^{ab}, \varphi_2^{ab}, \varphi_3^{ab})}^{1/2,0} + \text{tr} \gamma_{\theta^3}^a \text{tr} \gamma_{\theta^3}^{b,-1} I_{ab}^{\theta^3} \mathcal{A}_{v=1/2,(\varphi_1^{ab}, \varphi_2^{ab}, \varphi_3^{ab})}^{1/2,0} \right), \quad (35)$$

where  $I_{ab} = \prod_{k=1}^3 (n_k^a m_k^b - n_k^b m_k^a)$  is the intersection number between the factorizable D6-branes  $a$  and  $b$  and  $I_{ab}^{\theta^3}$  is the number of those intersections which are invariant under the  $\theta^3$  insertion, i.e. intersections localized at the  $\mathbb{Z}_2$  fixed points  $e_{ij}$  on  $T_1^2 \times T_2^2$  and with arbitrary position on  $T_3^2$ . One subtlety arises from the existence of the discrete Wilson lines: the  $\mathbb{Z}_2$  invariant intersections are counted with relative signs which come from the Wilson lines. The matrices  $\gamma_{\theta^3}$  are displayed below in section 3.2.3, eq. (39). For bulk branes,  $\text{tr} \gamma_{\theta^3}^a = N_a - N_a = 0$ , and  $\mathbb{Z}_2$  insertions give vanishing contributions to the annulus amplitude. For fractional branes  $a$ , the coefficient of the contribution from the  $\mathbb{I}$  insertion decreases by a factor of two, i.e. replace  $(2N_a) \rightarrow N_a$ , in accord with the expectation from the boundary state approach and  $\text{tr} \gamma_{\theta^3}^a$  is replaced by  $\tau_0^a N_a$  where  $\tau_0^a = \pm 1$  distinguishes the  $\mathbb{Z}_2$  eigenvalues of the two fractional branes  $\frac{1}{2}(\Pi_a^{\text{bulk}} \pm \Pi_a^{\text{ex}})$  forming a bulk brane.

For branes parallel on a 2-torus, in the above formula, the intersection number on the corresponding 2-torus is replaced by the appropriate lattice sum (62) and the oscillator expression is modified as explained in appendix C.3.

The annulus amplitude is sufficient to compute the massless spectrum of strings which are not invariant under the orientifold projection. This comprises the adjoint representations localized on a stack of identical branes or stuck at intersections of orbifold images as well as bifundamental representations at intersections of different branes  $a$  and  $b$ .

For  $N_a$  fractional branes  $a$  which are not their own  $\Omega\mathcal{R}$  image, the R sector annulus contributions containing adjoint representations are given by

$$\begin{aligned} \mathcal{A}_{aa}^R &= \frac{c}{24} \int_0^\infty \frac{dt}{t^3} \left( N_a^2 \mathcal{L}_1^{\mathcal{A},a} \mathcal{L}_2^{\mathcal{A},a} \mathcal{L}_3^{\mathcal{A},a} \mathcal{A}_{0,(0,0,0)}^{1/2,0} + (\tau_0^a)^2 N_a^2 \mathcal{L}_3^{\mathcal{A},a} \mathcal{A}_{v=1/2,(0,0,0)}^{1/2,0} \right) \\ &= \frac{c}{24} \int_0^\infty \frac{dt}{t^3} (16N_a^2 + \mathcal{O}(e^{-2\pi t})), \\ \mathcal{A}_{a(\Theta a)}^R &= \frac{c}{24} \int_0^\infty \frac{dt}{t^3} \left( N_a^2 I_{a(\Theta a)} \mathcal{A}_{0,(1/3,1/3,-2/3)}^{1/2,0} + (\tau_0^a)^2 N_a^2 I_{a(\Theta a)}^{\theta^3} \mathcal{A}_{v=1/2,(1/3,1/3,-2/3)}^{1/2,0} \right) \\ &= \frac{c}{24} \int_0^\infty \frac{dt}{t^3} \left( (2I_{a(\Theta a)} + 2I_{a(\Theta a)}^{\theta^3}) N_a^2 + \mathcal{O}(e^{-2\pi t/3}) \right), \\ \mathcal{A}_{a(\Theta^2 a)}^R &= \frac{c}{24} \int_0^\infty \frac{dt}{t^3} \left( N_a^2 I_{a(\Theta^2 a)} \mathcal{A}_{0,(-1/3,-1/3,2/3)}^{1/2,0} + (\tau_0^a)^2 N_a^2 I_{a(\Theta^2 a)}^{\theta^3} \mathcal{A}_{v=1/2,(-1/3,-1/3,2/3)}^{1/2,0} \right) \\ &= \frac{c}{24} \int_0^\infty \frac{dt}{t^3} \left( (2I_{a(\Theta^2 a)} + 2I_{a(\Theta^2 a)}^{\theta^3}) N_a^2 + \mathcal{O}(e^{-2\pi t/3}) \right). \end{aligned} \quad (36)$$

It follows that the gauge group with support on  $N_a$  identical branes wrapping  $\frac{1}{2}(\Pi_a^{\text{bulk}} \pm \Pi_a^{\text{ex}})$  is  $U(N_a)$ . The gauge sector preserves  $\mathcal{N} = 2$  supersymmetry, i.e. one multiplet in the adjoint representation is living on the worldvolume of the stack of branes. This multiplet carries the degrees of freedom which corresponds to a parallel displacement of the 1-cycle on the third torus. At each intersection of  $a$  with its orbifold images  $(\theta^k a)$ , one further chiral multiplet in the adjoint representation is stuck which is due to the fact that the orbifold images can recombine into a smooth cycle.

### 3.2.2 Symmetric and antisymmetric matter: Möbius strip

Arbitrary string configurations are not invariant under  $\Omega\mathcal{R}$ . However, some D6-branes can wrap the same 3-cycles as the O6-planes. In this case, the Möbius strip gives non-vanishing contributions to the gauge degrees of freedom and the resulting gauge group is special orthogonal.

Furthermore, strings can stretch between a brane  $a$  and an orbifold image in the orbit of the  $\mathcal{R}$  image  $a'$ . These strings provide for further antisymmetric or symmetric representations of the unitary gauge factor with support on  $a$ .

The only non-vanishing R sector contributions to the Möbius strip are of the form

$$\mathcal{M}_R = \frac{c}{24} \int_0^\infty \frac{dt}{t^3} \left\{ \text{Tr}_{\text{open}}^{R,aa'} (\Omega\mathcal{R}(\mathbb{I} + \theta^3)e^{-2\pi t L_0}) + \text{Tr}_{\text{open}}^{R,a(\theta a)'} (\Omega\mathcal{R}(\theta + \theta^4)e^{-2\pi t L_0}) + \text{Tr}_{\text{open}}^{R,a(\theta^2 a)'} (\Omega\mathcal{R}(\theta^2 + \theta^5)e^{-2\pi t L_0}) \right\}. \quad (37)$$

They can be rewritten in terms of oscillator contributions and eigenvalues  $\tau_k^a = \pm 1$  under  $\Omega\mathcal{R}\theta^k$  as follows,

$$\mathcal{M}_R = \frac{c}{24} \int_0^\infty \frac{dt}{t^3} \sum_{k=0}^2 \sum_{l=0,1} \tau_{k+3l}^a N_a I_{a(\theta^k a)'}^{\mathcal{R}\theta^{k+3l}} \mathcal{M}_{(\tilde{\varphi}_1 + (k+3l)/6, \tilde{\varphi}_2 + (k+3l)/6, \tilde{\varphi}_3 - (k+3l)/3)} \quad (38)$$

where  $\pi\tilde{\varphi}_k$  is the angle of brane  $a$  w.r.t. the  $\mathcal{R}$  invariant axis as described in section 2.5.1.  $I_{a(\theta^k a)'}^{\mathcal{R}\theta^{k+3l}}$  counts the number of intersections between  $a$  and  $(\theta^k a)'$  which are invariant under  $\mathcal{R}\theta^{k+3l}$ .

For example, let  $a$  and  $b$  be the fractional branes wrapping the bulk parts of the cycles on top of the O6-planes in the **AAB** model with wrapping numbers as displayed in table 2, i.e.  $\Pi_a = \frac{1}{2}(\rho_1 + \rho_2) + \frac{\tau_0^a}{2}(\varepsilon_1 + \tilde{\varepsilon}_1 + \varepsilon_2 + \tilde{\varepsilon}_2 + \varepsilon_3 + \tilde{\varepsilon}_3)$  and  $\Pi_b = \frac{3}{2}(\rho_1 + \rho_2) - \frac{\tau_0^b}{2}(\varepsilon_1 + \tilde{\varepsilon}_1 + \varepsilon_2 + \tilde{\varepsilon}_2 + \varepsilon_3 + \tilde{\varepsilon}_3)$  with  $\tau_0^{a,b} = \pm 1$  being the two possible  $\mathbb{Z}_2$  eigenvalues. The  $aa$  and  $bb$  strings support the gauge group  $SO(N_a) \times SO(N_b)$  and one chiral multiplet in the antisymmetric representation, **Anti** $_a + \text{Anti}_b$ . Furthermore, intersections of  $a$  with its orbifold images  $(\theta^k a)$  ( $k = 1, 2$ ) provide for three multiplets in **Anti** $_a$ , and  $b(\theta^k b)$  strings contribute 15 multiplets in **Anti** $_b$ . For  $\tau_0^a = \tau_0^b$ ,  $ab$  and  $a(\theta^2 b)$  strings carry three multiplets in  $(\mathbf{N}_a, \mathbf{N}_b)$ , and four multiplets in  $(\mathbf{N}_a, \mathbf{N}_b)$  live on the  $a(\theta b)$  strings. For  $\tau_0^a = -\tau_0^b$ , all sectors  $a(\theta^k b)$  give vanishing contributions to the spectrum. Observe that this spectrum can be compared to the one arising from the branes  $c$  and  $e$  in table 14. In the latter case, the discrete relative Wilson on  $T_1^2$  leads to a non-vanishing contribution to the spectrum although the  $\mathbb{Z}_2$  eigenvalues differ.

### 3.2.3 Computation of the open spectrum from Chan-Paton labels

The open string spectrum at fractional D6-branes can be computed in a similar way as for bulk branes using the decomposition into irreducible representations of the orbifold group as follows.<sup>4</sup>

One choice of matrices consistent with the fact that the D6-branes  $a$  and  $b$  at the end of section 3.2.2 carry orthogonal gauge factors and consequently  $\Omega\mathcal{R}$  has to preserve the  $\mathbb{Z}_2$

<sup>4</sup>See e.g. [68] for a recent review on such decompositions in orbifold compactifications.

eigenvalues is given by

$$\gamma_{\theta^3} = \begin{pmatrix} \mathbb{I}_N & 0 \\ 0 & -\mathbb{I}_N \end{pmatrix}, \quad \gamma_{\Omega\mathcal{R}} = \mathbb{I}_{2N}, \quad (39)$$

where  $N$  is the number of identical bulk branes. This choice confirms the global sign of the  $\Omega\mathcal{R}$  projection on exceptional cycles in table 3, i.e.  $\Omega\mathcal{R}$  acts merely as a permutation on exceptional 2-cycles but does not bring about any internal reflection of the blow-ups.

For an arbitrary kind of D6-branes wrapping a bulk 3-cycle which is not  $\Omega\mathcal{R}\theta^k$  invariant, the resulting gauge group is  $U(N)_1 \times U(N)_2$ . The two gauge factors belong to the two fractional branes whose superposition gives the bulk brane.

In particular, the  $aa$  strings decompose into  $\mathbb{Z}_2$  even massless states  $\psi_{-1/2}^I |0\rangle_{NS}$  for  $I = \mu, 3, \bar{3}$  and their superpartners which provide for the vector multiplet carrying the gauge group and one chiral multiplet in the adjoint representation. For  $I = 1, \bar{1}, 2, \bar{2}$  the massless states are  $\mathbb{Z}_2$  odd and correspond to strings stretching between the two fractional branes of opposite  $\mathbb{Z}_2$  eigenvalues forming a bulk brane.

In the example at the end of section 3.2.2, only one fractional cycle of each kind  $a$  and  $b$  occurs and therefore the  $\mathbb{Z}_2$  odd states do not contribute to the massless spectrum on the brane. The representations of states localized at the intersections  $a(\theta^k a)$  and  $b(\theta^k b)$  with  $k = 1, 2$  are computed from the fact that in this case the massless NS and R states are non-degenerate and  $\mathbb{Z}_2$  invariant. The bulk parts of the cycles  $a$  and  $(\theta^k a)$  intersect in three  $\mathbb{Z}_2$  invariant points while  $b$  and  $(\theta^k b)$  intersect in three  $\mathbb{Z}_2$  invariant points and 24 points which form pairs under  $\mathcal{R}$ . Similarly, the  $ab$  and  $a(\theta^2 b)$  massless states are non-degenerate and  $\mathbb{Z}_2$  invariant while  $a(\theta b)$  massless string states are twofold degenerate. By counting the respective intersections, the spectrum in section 3.2.2 is recovered.

## 4 Anomalies and Green-Schwarz mechanism

The closed string sector contains for all six different choices of lattice orientations the axion as untwisted RR scalar and five additional RR scalars from the  $\theta^3$  twisted sector. The number of vectors arising from the RR sectors depends on the lattice. The complete bosonic closed string spectrum is listed in table 5, the fermionic degrees of freedom follow from supersymmetry.

The axion and the five twisted RR scalars are those fields which participate in the generalized Green-Schwarz mechanism. Using the tables 1 and 3, the 3-cycles can be reexpressed in terms of  $\mathcal{R}$  even and  $\mathcal{R}$  odd linear combinations  $\eta_i$  and  $\chi_j$  ( $i, j = 0, \dots, 5$ ), respectively, with the property  $\eta_i \circ \chi_j = -4\delta_{ij}$  and all other intersections being trivial. The detailed form of these linear combinations depends on the choice of the lattice as listed in tables 6 and 7.

A general 3-cycle and its  $\mathcal{R}$  image can be rewritten in terms of the  $\mathcal{R}$  even and odd cycles as follows,

$$\Pi_a = \sum_{i=0}^5 (r_a^i \eta_i + s_a^i \chi_i), \quad \Pi_{a'} = \sum_{i=0}^5 (r_{a'}^i \eta_i - s_{a'}^i \chi_i), \quad (40)$$

with  $r_a^i, s_a^i$  multiples of one quarter. The RR tadpole cancellation condition (22) can be rephrased in terms of these coefficients as

$$\sum_b 2N_b \vec{r}_b = 4\vec{r}_{O6} \quad (41)$$

| Closed string spectrum $T^6/(\mathbb{Z}_6 \times \Omega\mathcal{R})$ |   |      |       |    |       |      |       |      |       |      |       |    |  |
|--|---|------|-------|----|-------|------|-------|------|-------|------|-------|----|--|
| lattice  | AAA   |      | AAB   |    | ABA   |      | ABB   |      | BBA   |      | BBB   |    |  |
| sector   | NSNS  | RR   | NSNS  | RR | NSNS  | RR   | NSNS  | RR   | NSNS  | RR   | NSNS  | RR |  |
| untwisted  | NSNS: Graviton + Dilaton + 10 scalars; RR: Axion + 1 vector |      |       |    |       |      |       |      |       |      |       |    |  |
| $\theta + \theta^5$  | 4 s.  | 1 v. | 6 s.  | —  | 4 s.  | 1 v. | 6 s.  | —    | 4 s.  | 1 v. | 6 s.  | —  |  |
| $\theta^2 + \theta^4$  | 20 s.   | 5 v. | 30 s. | —  | 18 s. | 6 v. | 24 s. | 3 v. | 20 s. | 5 v. | 30 s. | —  |  |
| $\theta^3$   | NSNS: 15 scalars; RR: 5 scalars + 1 vector                  |      |       |    |       |      |       |      |       |      |       |    |  |

Table 5: Closed string spectrum of  $T^6/(\mathbb{Z}_6 \times \Omega\mathcal{R})$ : Counting of the bosonic degrees of freedom. The fermionic degrees of freedom follow from supersymmetry. 1 s. corresponds to a real scalar while 1 v. denotes a massless vector with its two helicities.

| $\mathcal{R}$ even cycles for $T^6/\mathbb{Z}_6$ |                     |  |  |  |   |  |
|--|---------------------|--|--|--|---|--|
| lattice  | $\eta_0$            | $\eta_1$                                 | $\eta_2$                                 | $\eta_3$                                 | $\eta_4$  | $\eta_5$   |
| <b>AAA</b>                                       | $\rho_1$            | $\varepsilon_1$                          | $\varepsilon_2$                          | $\varepsilon_3$                          | $\varepsilon_4 + \varepsilon_5$                         | $-\tilde{\varepsilon}_4 - \varepsilon_5 + \tilde{\varepsilon}_5$ |
| <b>AAB</b>                                       | $\rho_1 + \rho_2$   | $\varepsilon_1 + \tilde{\varepsilon}_1$  | $\varepsilon_2 + \tilde{\varepsilon}_2$  | $\varepsilon_3 + \tilde{\varepsilon}_3$  | $-\tilde{\varepsilon}_4 - \varepsilon_5$                | $-\varepsilon_4 - \tilde{\varepsilon}_5$                         |
| <b>ABA</b>                                       | $\rho_1 + \rho_2$   | $\varepsilon_1$                          | $-\tilde{\varepsilon}_2$                 | $\varepsilon_5$                          | $\varepsilon_3 + \varepsilon_4$                         | $-\tilde{\varepsilon}_3 - \varepsilon_4 + \tilde{\varepsilon}_4$ |
| <b>ABB</b>                                       | $\rho_2$            | $\varepsilon_1 + \tilde{\varepsilon}_1$  | $\varepsilon_2 - 2\tilde{\varepsilon}_2$ | $\varepsilon_5 + \tilde{\varepsilon}_5$  | $-\tilde{\varepsilon}_3 - \varepsilon_4$                | $-\varepsilon_3 - \tilde{\varepsilon}_4$                         |
| <b>BBA</b>                                       | $\rho_2$            | $-\tilde{\varepsilon}_1$                 | $-\tilde{\varepsilon}_2$                 | $-\tilde{\varepsilon}_3$                 | $\varepsilon_4 - \varepsilon_5 + \tilde{\varepsilon}_5$ | $-\tilde{\varepsilon}_4 - \tilde{\varepsilon}_5$                 |
| <b>BBB</b>                                       | $-\rho_1 + 2\rho_2$ | $\varepsilon_1 - 2\tilde{\varepsilon}_1$ | $\varepsilon_2 - 2\tilde{\varepsilon}_2$ | $\varepsilon_3 - 2\tilde{\varepsilon}_3$ | $\varepsilon_4 - \varepsilon_5$                         | $-\tilde{\varepsilon}_4 + \varepsilon_5 - \tilde{\varepsilon}_5$ |

Table 6:  $\mathcal{R}$  even cycles for  $T^6/(\mathbb{Z}_6 \times \Omega\mathcal{R})$ .

with  $\vec{r}_{O6} = (r_{O6}^0, 0, 0, 0, 0, 0)^T$  and  $r_{O6}^0$  as read off from table 2. Using the fact that the intersection number of two arbitrary 3-cycles is given by  $\Pi_a \circ \Pi_b = 2(-\vec{r}_a \cdot \vec{s}_b + \vec{s}_a \cdot \vec{r}_b)$ , and multiplying (41) by  $2\vec{s}_a$  leads to

$$\begin{aligned}
0 &= 4N_a \vec{s}_a \cdot \vec{r}_a - 8\vec{s}_a \cdot \vec{r}_{O6} + 4 \sum_{b \neq a} N_b \vec{s}_a \cdot \vec{r}_b \\
&= N_a \Pi_a \circ \Pi_{a'} - 4\Pi_a \circ \Pi_{O6} + \sum_{b \neq a} N_b (\Pi_a \circ \Pi_b + \Pi_a \circ \Pi_{b'}) .
\end{aligned} \tag{42}$$

As in the toroidal orientifold models with intersecting D6-branes [20], equation (42) shows manifestly that the RR tadpole cancellation conditions imply the disappearance of all cubic gauge anomalies of the generic spectrum listed in table 4 and impose analogous conditions for matter charged under  $SU(2)$  and  $U(1)$  factors.

| $\mathcal{R}$ odd cycles for $T^6/\mathbb{Z}_6$ |                     |   |   |   |  |   |
|---|---------------------|---|---|---|--|---|
| lattice   | $\chi_0$            | $\chi_1$                                  | $\chi_2$                                  | $\chi_3$                                  | $\chi_4$   | $\chi_5$  |
| <b>AAA</b>                                      | $-\rho_1 + 2\rho_2$ | $-\varepsilon_1 + 2\tilde{\varepsilon}_1$ | $-\varepsilon_2 + 2\tilde{\varepsilon}_2$ | $-\varepsilon_3 + 2\tilde{\varepsilon}_3$ | $\tilde{\varepsilon}_4 - \varepsilon_5 + \tilde{\varepsilon}_5$  | $\varepsilon_4 - \varepsilon_5$                         |
| <b>AAB</b>                                      | $-\rho_1 + \rho_2$  | $-\varepsilon_1 + \tilde{\varepsilon}_1$  | $-\varepsilon_2 + \tilde{\varepsilon}_2$  | $-\varepsilon_3 + \tilde{\varepsilon}_3$  | $\varepsilon_4 - \tilde{\varepsilon}_5$                          | $-\tilde{\varepsilon}_4 + \varepsilon_5$                |
| <b>ABA</b>                                      | $-\rho_1 + \rho_2$  | $-\varepsilon_1 + 2\tilde{\varepsilon}_1$ | $2\varepsilon_2 - \tilde{\varepsilon}_2$  | $-\varepsilon_5 + 2\tilde{\varepsilon}_5$ | $\tilde{\varepsilon}_3 - \varepsilon_4 + \tilde{\varepsilon}_4$  | $\varepsilon_3 - \varepsilon_4$                         |
| <b>ABB</b>                                      | $-2\rho_1 + \rho_2$ | $-\varepsilon_1 + \tilde{\varepsilon}_1$  | $\varepsilon_2$                           | $-\varepsilon_5 + \tilde{\varepsilon}_5$  | $\varepsilon_3 - \tilde{\varepsilon}_4$                          | $-\tilde{\varepsilon}_3 + \varepsilon_4$                |
| <b>BBA</b>                                      | $-2\rho_1 + \rho_2$ | $2\varepsilon_1 - \tilde{\varepsilon}_1$  | $2\varepsilon_2 - \tilde{\varepsilon}_2$  | $2\varepsilon_3 - \tilde{\varepsilon}_3$  | $\tilde{\varepsilon}_4 - \tilde{\varepsilon}_5$                  | $\varepsilon_4 - \tilde{\varepsilon}_4 + \varepsilon_5$ |
| <b>BBB</b>                                      | $-\rho_1$           | $\varepsilon_1$                           | $\varepsilon_2$                           | $\varepsilon_3$                           | $-\varepsilon_4 + \tilde{\varepsilon}_4 - \tilde{\varepsilon}_5$ | $\varepsilon_4 + \varepsilon_5$                         |

Table 7:  $\mathcal{R}$  odd cycles for  $T^6/(\mathbb{Z}_6 \times \Omega\mathcal{R})$ .

The mixed gauge anomalies are of the form

$$\mathcal{A}_{U(1)_a - SU(N_b)^2} = 4\vec{s}_a \cdot \left( \vec{r}_b N_a + \delta_{ab} \left( \sum_c N_c \vec{r}_c - 2\vec{r}_{O6} \right) \right) C_2(N_b). \quad (43)$$

The inner bracket in (43) vanishes upon RR tadpole cancellation. The remaining part which is also present for  $a \neq b$  is compensated by the generalized Green-Schwarz couplings as follows. Six linearly independent  $\Omega\mathcal{R}$  even RR scalars and their dual two-forms can be defined as the pull back of the ten dimensional  $\Omega$  even 3-form and the  $\Omega$  odd 5-form over the  $\mathcal{R}$  even and  $\mathcal{R}$  odd 3-cycles, respectively,

$$\tilde{\phi}_i = (4\pi^2 \alpha')^{-3/2} \int_{\eta_i} C_3, \quad \tilde{B}_2^i = (4\pi^2 \alpha')^{-3/2} \int_{\chi_i} C_5. \quad (44)$$

The axion of table 5 corresponds to  $\tilde{\phi}_0$  while the remaining scalars  $\tilde{\phi}_1, \dots, \tilde{\phi}_5$  represent the five RR scalars from the  $\theta^3$  twisted sector.

The four dimensional effective couplings to the gauge fields are determined by the coefficients of the 3-cycles in (40),

$$N_b \sum_{i=0}^5 2r_b^i \int_{M_4} \tilde{\phi}_i \text{tr} F_b \wedge F_b, \quad N_a \sum_{i=0}^5 2s_a^i \int_{M_4} \tilde{B}_i \wedge \text{tr} F_a, \quad (45)$$

the factor of two stemming from the couplings to branes  $a$  as well as their images  $a'$ . The couplings in (45) obviously match those in (43) and thus provide for the cancellation of mixed gauge anomalies.

In order for a  $U(1)$  factor  $Q = \sum_a x_a Q_a$  to remain massless, the couplings to all two-forms have to vanish, i.e. the coefficients  $x_a$  have to fulfill

$$\sum_a x_a N_a \vec{s}_a = 0. \quad (46)$$

In a generic model, at most six Abelian gauge factors can acquire a mass. However, in a supersymmetric set-up all couplings to  $\tilde{B}_0$  vanish and only up to five Abelian factors can become massive.

The non-anomalous  $U(1)$ s can also be calculated directly from the homological cycles by determining the kernel of the matrix [14, 15]

$$M_{aI} = N_a (v_a^I - v_a^{I'}), \quad (47)$$

where  $v_a^I$  and  $v_a^{I'}$  are just the twelve coefficients of the homological basis and the  $\Omega\mathcal{R}$ -mirror, respectively;  $a$  runs over all stacks of branes.

## 5 Supersymmetric models

After having specified the RR tadpole and supersymmetry conditions, it is now possible to search for concrete configurations of fractional cycles fulfilling these conditions. We will proceed in the usual way for a certain number  $r$  of stacks, each consisting of  $N_r$  branes. Our main aim is to find a phenomenologically appealing supersymmetric 3 generation model, ideally without any exotic chiral matter as compared to the standard model.

The guiding model for our considerations will be the non-supersymmetric standard model on the toroidal orientifold of [20] which might also allow for a supersymmetric extension. It has the two main features that firstly, it only contains exactly the standard model matter as chiral matter (plus right handed neutrinos) and secondly, only in bifundamental representations of the gauge groups. This model is realized on four stacks plus possibly hidden branes (which do not intersect with the standard model branes). The second different possibility to realize the standard model from [23] does not have a supersymmetric extension on the  $\mathbb{Z}_6$ -orientifold for the following reason: in this model, the right handed  $u$ ,  $c$  and  $t$  quarks have been realized in the antisymmetric representation of the  $U(3)$  brane and it was not allowed to have any symmetric representations of this gauge factor. In the present case, the intersection of any brane cycle  $\Pi_a$  with the orientifold plane  $\Pi_{O6}$  has to vanish for a supersymmetric model, i.e.  $\Pi_a \circ \Pi_{O6} = 0$ . But according to table 4, this just means that the number of symmetric and antisymmetric representations on a certain brane are always the same.

In the past, the model building approaches often have been rather non-systematic, a fact that we will try to avoid here. To do so, a computer program has been set up in order to first calculate the configurations in terms of wrapping numbers  $n$  and  $m$  which fulfil the untwisted RR tadpole conditions and the supersymmetry conditions at the same time, where we have to keep in mind that only the untwisted RR tadpole conditions get a contribution from the orientifold planes.

Having specified all such configurations in a certain range of wrapping numbers, all possible fractional cycles are constructed after a reduction to one representant of the orbit. This of course has to be done according to the specific fixed points that the particular fractional brane passes through. The possible cycles can be determined from table 23, where we have allowed a displacement of the branes from the origin by

$$\sum_{i=1}^4 \sigma_i \pi_i \quad \text{with} \quad \sigma_i \in \left\{ 0, \frac{1}{2} \right\} \quad (48)$$

on the first two  $T^2$ , according to the discussion in the preceding sections. For every given configuration of wrapping numbers fulfilling the RR tadpole conditions in the untwisted part, this procedure allows for a number of  $16 \cdot 2^3 = 128$  different cycles according to equation (28) and table 23 for every stack. This enhances the model building possibilities by a factor of

| $(I_{ab}, I_{ab'})$ |                  |
|---------------------|------------------|
| $(0, 0)$            | $(\pm 1, \pm 1)$ |
| $(\pm 2, \pm 2)$    | $(\pm 3, \pm 3)$ |
| $(\pm 5, \pm 5)$    | $(0, \pm 1)$     |
| $(\pm 1, 0)$        | $(0, \pm 3)$     |
| $(\pm 3, 0)$        | $(\pm 1, \pm 3)$ |
| $(\pm 3, \pm 1)$    |                  |

Table 8: All possible intersection numbers  $(I_{ab}, I_{ab'})$  between two stacks of branes  $a$  and  $b$  for intersections with only bifundamental representations of the gauge group.

$128^r$  (where  $r$  again is the number of stacks) as compared to the case of constructions without fractional cycles (like in the  $\mathbb{Z}_3$  orientifold of [23]). The reader should be reminded that the fulfillment of the untwisted RR tadpole equation actually does not depend on the specific choices of wrapping numbers  $n$  and  $m$  for every stack of branes, but only on the corresponding coefficients of the two homological cycles  $Y_a$  and  $Z_a$  which are defined in equation (6). In contrast, the construction of twisted cycles does depend on the numbers  $n$  and  $m$ , but actually only on the oddness and evenness of the wrapping numbers on the first two tori. These two facts allow for a more effective and evolved computer algorithm to handle the amount of computation.

To get started, we will look for all generally possible two stack configurations (which for now shall be denoted  $a$  and  $b$ ). We will not require to fulfil the RR tadpole equation at this point, therefore we do not have to specify the size  $N_r$  for any of these two stacks. In this way we get the most general intersection numbers which – most optimistically – are possible in any  $\mathbb{Z}_6$  orientifold construction (with more than one stack). These intersection numbers make up a finite set, if we insist on constructions without anti-D-branes, simply because every D-brane gives a positive contribution which never should be larger than the absolute value of the contribution from the orientifold plane. This gives an upper bound on  $Y_a$  and  $Z_a$  if one assumes the smallest possible stacksize of  $N_a = 1$ . The computation shows that the possibilities completely agree on all possible tori. They are listed in table 8 for the case that the intersections of the two branes with themselves and their orientifold mirror brane are vanishing, i.e.  $I_{aa} = I_{aa'} = I_{bb} = I_{bb'} = 0$ <sup>5</sup>. This means that we require that there are no symmetric and antisymmetric representations in the corresponding open string sectors. Another computation shows that exactly the same intersections are still possible if we additionally insist on  $\mathcal{N} = 1$  supersymmetry on both stacks.

We can already see from this table, that an identical construction of the standard model spectrum to the one in [20] also will not be possible: one cannot get a pair of intersection numbers between two stacks of the form  $(I_{ab}, I_{ab'}) = (1, 2)$ . In the model in [20], this possibility was necessary in order to realize the three generations of left-handed quarks as two  $SU(2)$  doublets and one antidoublet. In this way, no additional (w.r.t. the standard model)  $SU(2)$  lepton doublets were required in order to cancel the  $U(2)$  anomaly in the effective 4-dimensional gauge sector.

This problem seems to persist in the construction on the  $\mathbb{Z}_6$  orientifold, but later we will see how it actually can be overcome and that we can even profit from this fact. At this point, it just shall be mentioned that this might only be a problem in a construction with four observable

<sup>5</sup>In fact, the intersection number of any brane with itself vanishes automatically in four dimensions.

| stack | $(n_I, m_I)$            | homology cycle  | chiral spectrum  |
|-------|-------------------------|---|--|
| U(3)  | $(-3, 1; -3, 2; -1, 1)$ | $\Pi_1 = \frac{1}{2}(7\rho_2 - \varepsilon_1 - \varepsilon_3 + 2\tilde{\varepsilon}_1 + \tilde{\varepsilon}_3 + \tilde{\varepsilon}_5)$ | $2 \times (\bar{\mathbf{3}}, \mathbf{3})$                            |
|       |                         | $\Pi'_1 = \frac{1}{2}(7\rho_2 + 2\varepsilon_1 + \varepsilon_4 + \varepsilon_5 - \tilde{\varepsilon}_1 - \tilde{\varepsilon}_4)$        | $1 \times (\mathbf{3}_A, 1), 1 \times (\mathbf{6}_S, 1)$             |
| U(3)  | $(0, -1; 0, 1; -1, 1)$  | $\Pi_2 = \frac{1}{2}(\rho_2 - 2\varepsilon_1 - \varepsilon_4 - \varepsilon_5 + \tilde{\varepsilon}_1 + \tilde{\varepsilon}_4)$          | $1 \times (1, \bar{\mathbf{3}}_A), 1 \times (1, \bar{\mathbf{6}}_S)$ |
|       |                         | $\Pi'_2 = \frac{1}{2}(\rho_2 + \varepsilon_1 + \varepsilon_3 - 2\tilde{\varepsilon}_1 - \tilde{\varepsilon}_3 - \tilde{\varepsilon}_5)$ |  |

Table 9: The wrapping numbers and homology cycles of the D6-branes in a 2-stack model containing chiral matter.

intersecting (plus hidden) stacks.

Before coming to the most interesting 5 stack configurations, we will shortly mention some results on 2, 3 and 4 stack configurations and how they automatically point towards a 5 stack model.

### 5.1 2, 3 and 4 stack configurations

Even with 2 stacks of various stacksizes, already non-trivial models which fulfill the RR tadpole cancellation conditions and carry matter in bifundamental representations can be obtained. But in all such models on all six different tori, the stacksize of both stacks has to agree. Besides, there also exists matter in the symmetric and antisymmetric representation of at least one gauge factor and furthermore, only even intersection numbers are possible. This means that the number of bifundamental representations is always even, too. A typical example for  $N_a = N_b = 3$  on the **AAA**-torus is given in table 9.

These limitations can be explained by the simple fact that the twisted homological cycles plus their  $\mathcal{R}$ -mirrors have to be exactly opposite to each other for the two stacks. Therefore, one cannot obtain any 3-generation model like the SU(5)-GUT model in [23] and one has to allow for at least 3 stacks for a phenomenologically appealing model.

There is a simple possibility how to sort out right from the start which stacksizes are able to give valid models and which are not. Indeed, only the first two components of the RR-tadpole equation (22) which do not depend on the construction of fractional cycles, are already enough to rule out most of the possibilities, because if there are no solutions for a given stacksize, the fractional cycles cannot change this. On the other hand, if there are solutions of the untwisted RR-tadpole components, it is not ensured that the twisted RR-tadpole components also admit solutions.

Using 3 stacks, it turns out that there are solutions of the untwisted components of the RR-tadpole equation for the most appealing given stacksizes  $N_1 = 3, N_2 = 2, N_3 = 1$ . After the construction of fractional cycles, it is observed that all existing solutions with chiral matter contain antisymmetric (and by this also symmetric) representations of the gauge group, but it is possible to have this only on the most ‘harmless’  $N_3 = 1$ -stack. Requiring this additional constraint, it is found that just three bifundamental representations between the  $U(3)$ - and the  $U(2)$ -stack are not possible, so one cannot obtain 3 left-handed quark generations.

If one turns over to 4 stacks, it is observed quickly from the untwisted components of the RR-tadpole equation that the most favorable configuration  $N_1 = 3, N_2 = 2, N_3 = 1, N_4 = 1$  does not produce any solutions. However, the two configurations  $N_1 = 4, N_2 = 2, N_3 = 1, N_4 = 1$  and  $N_1 = 3, N_2 = 2, N_3 = 2, N_4 = 1$  which still might be acceptable, provide for solutions. Requiring again no antisymmetric representations on the first brane, it is observed that just on

the **ABB**-torus, there exist solutions with 3 bifundamental representations between the first and the second brane, i.e. there exist 3 left-handed quarks. This seems rather nice, but in the further investigation of these models it turns out that there are always more than three  $U_R$  and  $D_R$  quarks in the  $(\bar{\mathbf{3}}, 1)$  representation of  $SU(3) \times SU(2)$  localized at intersections between the  $U(3)$  and any one of the  $U(1)$  stacks.

From all this, we have to conclude that there have to be at least five stacks of branes to obtain 3 quark generations and it indeed turns out that with this number of stacks, it is possible to obtain a very appealing class of phenomenological models which will be introduced in the following section.

## 5.2 5 stack configurations

For the search of 5 stack models, we cannot proceed exactly in the same way as for 4 stack configurations, because it would require much too much computer power to go through all possible constructions with fractional cycles. Therefore, we will alter our approach in the following way: we fix the stacksize on the first three stacks to be  $N_a = 3$ ,  $N_b = 2$  and  $N_c = 1$ . Then we require from the beginning that firstly, there are no (anti-)symmetric representations of the  $U(3)$  gauge factor, secondly, that the absolute value of intersection numbers are  $|I_{ab} + I_{ab'}| \equiv 3$  and  $|I_{ac} + I_{ac'}| \equiv 6$ . This just means that we demand (up to conjugation) three left-handed quark generations in the bifundamental representation  $(\mathbf{3}, \mathbf{2})$  and that the sum of  $U_R$  and  $D_R$  quark generations in the representation  $(\bar{\mathbf{3}}, 1)$  has to be six.

For all homological cycles fulfilling this condition, we now search for a variable stacksize on the 4th and 5th torus if (and for which  $N_d, N_e$ ) the two untwisted components of the RR-tadpole equations can be fulfilled. For the remaining possibilities, we construct all possible fractional cycles also on the 4th and 5th stack and then look for the spectra which are possible. At this point, there is a rather miraculous observation we have made: if we furthermore require that there are no (anti-)symmetric representations of any gauge factor, there remains exactly *one* class of models with a given chiral spectrum.<sup>6</sup> This model has the two stacksizes  $N_d = N_e = 1$ . The same observation has been made on all three possible tori which give results at all (namely the **AAB**, **ABA** and **ABB** tori) and the chiral spectra of these models all agree. Even more astonishingly, this model resembles almost exactly the non-supersymmetric model of [20] with regard to the chiral spectrum. There is just one difference: on the 5th stack  $e$ , there are three additional bifundamental representations. At this point, we should make another remark, being that all nonvanishing intersection numbers have an absolute value 3, this seems to be a very aesthetical feature of this model and most likely could be understood in more depth directly from the  $\mathbb{Z}_6$  symmetry.

There is another observation which completely agrees on the whole class of possibilities: the third and fifth homological cycles are  $\Omega\mathcal{R}$ -invariant. A detailed calculation shows that they both indeed are  $SO(2)$ -stacks. The chiral spectrum of this class of models is shown in table 10 for an example on the **AAB** torus.

The fact that we have two  $SO(2)$ - instead of  $U(1)$ -stacks is not a problem, because it just means that the two fractional branes coincide with their  $\Omega\mathcal{R}$ -mirror branes. In the non-chiral spectrum there is the adjoint representation of both gauge factors, being related to the unconstrained distance between the two branes and their mirrors on  $T_3^2$ . If one gives a VEV

---

<sup>6</sup>This statement is valid up to an overall minus sign of the intersection numbers, an exchange of the so-far equivalent 4th and 5th stack and an exchange between the general sectors  $xy$  and  $xy'$ , all leading to the same massless spectrum. The same result was found in [20].

| Chiral spectrum of 5 stack models with $N_a = 3, N_b = 2, N_c = N_d = N_e = 1$ |        |  |       |       |       |                        |
|--|--------|--|-------|-------|-------|------------------------|
|  | sector | $SU(3)_a \times SU(2)_b \times SO(2)_c \times SO(2)_e$ | $Q_a$ | $Q_b$ | $Q_d$ | $\frac{1}{3}Q_a + Q_d$ |
| $Q_L$  | $ab'$  | $3 \times (\bar{\mathbf{3}}, \mathbf{2}; 1, 1)$        | -1    | -1    | 0     | $-\frac{1}{3}$         |
| $U_R, D_R$   | $ac$   | $3 \times (\mathbf{3}, 1; \mathbf{2}, 1)$              | 1     | 0     | 0     | $\frac{1}{3}$          |
| $L$  | $bd'$  | $3 \times (1, \mathbf{2}; 1, 1)$                       | 0     | 1     | 1     | 1                      |
| $E_R, N_R$   | $cd$   | $3 \times (1, 1; \mathbf{2}, 1)$                       | 0     | 0     | -1    | -1                     |
|  | $be$   | $3 \times (1, \mathbf{2}; 1, \mathbf{2})$              | 0     | 1     | 0     | 0                      |

Table 10: Chiral spectrum of the model class with gauge group  $SU(3)_a \times SU(2)_b \times SO(2)_c \times U(1)_d \times SO(2)_e \times U(1)_a \times U(1)_b$ .

to these fields, then the branes and their mirrors are distinguishable and the gauge group is a  $U(1)$  instead of the  $SO(2)$  which indeed has the same rank. Then any bifundamental of the type  $(\mathbf{3}, \mathbf{2})$ , where the  $\mathbf{3}$  comes for instance from a  $U(3)$  and the  $\mathbf{2}$  from the  $SO(2)$ , splits up into a  $(\mathbf{3}, 1)$  and a  $(\mathbf{3}, -1)$ , where 1 and  $-1$  now are the  $U(1)$ -charges. After this transition, the  $U_R$ - and  $D_R$ -quarks (and the  $E_R$  and  $N_R$ ) are distinguishable as usual by their opposite  $U(1)$  charge.

Beside these common properties, the non-chiral spectrum which has been calculated according to the lines of section 3 disagrees for different models on just one and also between different tori. This is well understandable, because it does not only depend on the homology, but also on the geometrical properties of the branes and the choice of the lattice. In the next section, we will discuss two different explicit examples of this class of models in more detail.

|           | $(n_I, m_I)$            | $(\sigma_1, \sigma_2, \sigma_3, \sigma_4)$ | $(\tau_1, \tau_2)$ | $\mathbb{Z}_2$ |
|-----------|-------------------------|--|--------------------|----------------|
| $N_a = 3$ | $(-2, 1; -1, 2; -2, 1)$ | $(0, 0, 0, 0)$                             | $(0, 0)$           | —              |
| $N_b = 2$ | $(-1, 0; -1, 1; -1, 2)$ | $(0, 0, 0, 0)$                             | $(1, 0)$           | +              |
| $N_c = 1$ | $(-2, 1; -2, 1; -1, 2)$ | $(0, 0, 0, 0)$                             | $(1, 0)$           | +              |
| $N_d = 1$ | $(-1, 0; -1, 1; -1, 2)$ | $(0, 0, 0, 0)$                             | $(0, 0)$           | —              |
| $N_e = 1$ | $(-1, 1; -1, 1; -2, 1)$ | $(0, 0, 0, 0)$                             | $(0, 0)$           | —              |

Table 11: The setup of the D6-branes in the 5 stack model on the **AAB** torus.

| homology cycles   | intersections |                |
|---|---------------|----------------|
| $\Pi_a = \frac{1}{2}(3\rho_1 + 3\rho_2 - \varepsilon_1 + 2\varepsilon_2 - \varepsilon_5 + 2\tilde{\varepsilon}_1 - \tilde{\varepsilon}_2 + 2\tilde{\varepsilon}_5)$ | $I_{ab} = 0$  | $I_{ab'} = -3$ |
| $\Pi_b = \frac{1}{2}(\rho_1 + \rho_2 + \varepsilon_1 + 2\varepsilon_2 + \varepsilon_5 - 2\tilde{\varepsilon}_1 - \tilde{\varepsilon}_2 - 2\tilde{\varepsilon}_5)$   | $I_{ac} = 3$  | $I_{ac'} = 3$  |
| $\Pi_c = \frac{1}{2}(3\rho_1 + 3\rho_2 + \varepsilon_1 - \varepsilon_2 + \varepsilon_3 + \tilde{\varepsilon}_1 - \tilde{\varepsilon}_2 + \tilde{\varepsilon}_3)$    | $I_{bd} = 0$  | $I_{bd'} = 3$  |
| $\Pi_d = \frac{1}{2}(\rho_1 + \rho_2 + \varepsilon_1 - 2\varepsilon_2 + \varepsilon_5 - 2\tilde{\varepsilon}_1 + \tilde{\varepsilon}_2 - 2\tilde{\varepsilon}_5)$   | $I_{cd} = 3$  | $I_{cd'} = -3$ |
| $\Pi_e = \frac{1}{2}(\rho_1 + \rho_2 - \varepsilon_1 - \varepsilon_2 - \varepsilon_3 - \tilde{\varepsilon}_1 - \tilde{\varepsilon}_2 - \tilde{\varepsilon}_3)$      | $I_{be} = 3$  | $I_{be'} = 3$  |

Table 12: The homology cycles and intersection numbers (all other intersection numbers vanishing) of the D6-branes in the 5 stack model on the **AAB** torus.

## 6 The Supersymmetric Standard model

### 6.1 The model on the AAB torus

The explicit configuration that shall be discussed in this section is given in table 11, the homological cycles and intersection numbers are listed in table 12. After the displacement of the third and fifth stack on the third 2-torus (as discussed in the preceding section), the chiral spectrum takes the form as shown in table 13. We can immediately calculate which  $U(1)$  factors remain massless after applying the Green-Schwarz mechanism which is discussed in detail in section 4. The result is that one obtains three  $U(1)$ s which are free of triangle anomalies, being  $Q_{B-L} = -\frac{1}{3}Q_a - Q_d$ ,  $Q_c$  and  $Q_e$ . As in similar constructions, the first one is the  $B - L$  symmetry,  $Q_c$  is twice the third component of the right-handed weak isospin.  $Q_e$  is an additional  $U(1)$  symmetry under which none of the standard model particles transforms, only the two additional fields.

Also the linear combination

$$Q_Y = -\frac{1}{6}Q_a + \frac{1}{2}Q_c - \frac{1}{2}Q_d \quad (49)$$

is massless, being the hypercharge  $Y$ . Every chiral field has the correct quantum numbers (for both hypercharge and  $B - L$  symmetry), the only mystical one being the two additional fields at the  $be$  and  $be'$  intersections. Actually, these two kinds of fields have the right quantum numbers to be the supersymmetric standard model partners of the Higgs fields with a vanishing hypercharge,  $H$  and  $\bar{H}$ .<sup>7</sup> The only problem in the present construction is the fact that these

<sup>7</sup>The hypercharge could also be defined with an additional factor of  $-1/2Q_e$ , then the two additional kinds of fields would have the more familiar opposite hypercharge  $-1/2$  and  $1/2$ .

| Chiral spectrum of 5 stack model on AAB torus |        |   |       |       |       |       |       |                |                |  |
|---|--------|---|-------|-------|-------|-------|-------|----------------|----------------|--|
|   | sector | $SU(3)_a \times SU(2)_b$                  | $Q_a$ | $Q_b$ | $Q_c$ | $Q_d$ | $Q_e$ | $Q_{B-L}$      | $Q_Y$          |  |
| $Q_L$   | $ab'$  | $3 \times (\bar{\mathbf{3}}, \mathbf{2})$ | -1    | -1    | 0     | 0     | 0     | $\frac{1}{3}$  | $\frac{1}{6}$  |  |
| $U_R$   | $ac$   | $3 \times (\mathbf{3}, 1)$                | 1     | 0     | -1    | 0     | 0     | $-\frac{1}{3}$ | $-\frac{2}{3}$ |  |
| $D_R$   | $ac'$  | $3 \times (\mathbf{3}, 1)$                | 1     | 0     | 1     | 0     | 0     | $-\frac{1}{3}$ | $\frac{1}{3}$  |  |
| $L$   | $bd'$  | $3 \times (1, \mathbf{2})$                | 0     | 1     | 0     | 1     | 0     | -1             | $-\frac{1}{2}$ |  |
| $E_R$   | $cd$   | $3 \times (1, 1)$                         | 0     | 0     | 1     | -1    | 0     | 1              | 1              |  |
| $N_R$   | $cd'$  | $3 \times (1, 1)$                         | 0     | 0     | -1    | -1    | 0     | 1              | 0              |  |
|   | $be$   | $3 \times (1, \mathbf{2})$                | 0     | 1     | 0     | 0     | -1    | 0              | 0              |  |
|   | $be'$  | $3 \times (1, \mathbf{2})$                | 0     | 1     | 0     | 0     | 1     | 0              | 0              |  |

Table 13: Chiral spectrum of the model class with gauge group  $SU(3)_a \times SU(2)_b \times U(1)_a \times U(1)_b \times U(1)_c \times U(1)_d \times U(1)_e$ .

bifundamental fields do not stretch from the second stack to the  $c$ -brane, but to the  $e$ -brane, and therefore do not give rise to the standard Yukawa couplings.

But the problem at first sight can be overcome as well. It is known that in many cases a gauge breaking where two unitary gauge groups are broken to the diagonal subgroup is possible, in our case the breaking  $U(1)_c \times U(1)_e \rightarrow U(1)_C$  would be needed. In the language of D-branes, this requires a brane recombination mechanism which in some cases can be understood in the effective field theory just as a Higgs effect. We will explain in the following why this is exactly the case for the present model.

If two stacks of D-branes preserve a common  $\mathcal{N} = 2$  supersymmetry, then a massless hypermultiplet being localized at the intersection indicates that there is a possible deformation of the two stacks into just one recombined one. In our case, which is similar to the one described in [36], two factorizable branes can only preserve a common  $\mathcal{N} = 2$  supersymmetry if they are parallel on one of the three tori. To understand this for our concrete model, we have to take a look at the non-chiral spectrum. This has been calculated for the concrete model of table 11 as described in section 3 and the result is shown in table 14.

From this table, we can immediately see that the necessary hypermultiplets are indeed existing, being the ones in the sector between the  $c$  and  $e$ -brane. If we take a closer look at the computation and for a moment distinguish between the different orbifold images under the  $\theta$  action<sup>8</sup>, we observe that the two hypermultiplets are not in the  $ce$  sector, but in the  $c$  ( $\theta^2 e$ ) sector. In this sector, the branes  $c$  and  $(\theta^2 e)$  are indeed parallel on the third torus, see figure 2. Therefore, we can recombine in this way the  $c$  with the  $(\theta^2 e)$ -brane (and at the same time the  $(\theta c)$  with the  $e$  brane and the  $(\theta^2 c)$  with the  $(\theta e)$  brane) by giving a VEV to the two hypermultiplets in the following way: it is possible to understand the recombination as a Higgs effect in the  $\mathcal{N} = 2$  effective theory, if there exists a flat direction  $\langle h_1 \rangle = \langle h_2 \rangle$  in the D-term

<sup>8</sup>Of course, in the end we have to sum over all  $\theta$  images such that the result is invariant under the orbifold action.

| Non-chiral massless and light open spectrum, <b>AAB</b> on $T^6/(\mathbb{Z}_6 \times \Omega\mathcal{R})$ |  |                   |        |  |                   |
|--|--|-------------------|--------|--|-------------------|
| sector   | $U(3)_a \times U(2)_b(Q_c, Q_d, Q_e)$                      | $\sqrt{\alpha'}m$ | sector | $U(3)_a \times U(2)_b(Q_c, Q_d, Q_e)$        | $\sqrt{\alpha'}m$ |
| $aa$   | $16 \times (\mathbf{9}, 1)_{0,0,0}$                        | 0                 | $ad'$  | $6 \times [(\mathbf{3}, 1)_{0,1,0} + h.c.]$  | 0                 |
| $bb$   | $4 \times (1, \mathbf{4})_{0,0,0}$                         | 0                 |        | $(\mathbf{3}, 1)_{0,1,0} + h.c.$             | $\Sigma_{ad'}$    |
| $cc$   | $16 \times (1, 1)_{0,0,0}$                                 | 0                 | $ae$   | $6 \times [(\mathbf{3}, 1)_{0,0,-1} + h.c.]$ | 0                 |
| $dd$   | $4 \times (1, 1)_{0,0,0}$                                  | 0                 |        | $(\mathbf{3}, 1)_{0,0,-1} + h.c.$            | $\Sigma_{ae}$     |
| $ee$   | $4 \times (1, 1)_{0,0,0}$                                  | 0                 | $ae'$  | $6 \times [(\mathbf{3}, 1)_{0,0,1} + h.c.]$  | 0                 |
| $aa'$  | $9 \times [(\mathbf{3}_A, 1)_{0,0,0} + h.c.]$              | 0                 |        | $(\mathbf{3}, 1)_{0,0,1} + h.c.$             | $\Sigma_{ae'}$    |
|  | $5 \times [(\mathbf{3}_A, 1)_{0,0,0} + h.c.]$              | $\Sigma_{aa'}$    | $bc$   | $6 \times [(1, \mathbf{2})_{-1,0,0} + h.c.]$ | 0                 |
| $bb'$  | $3 \times [(1, \mathbf{1}_A)_{0,0,0} + h.c.]$              | 0                 |        | $(1, \mathbf{2})_{-1,0,0} + h.c.$            | $\Sigma_{bc}$     |
|  | $(1, \mathbf{1}_A)_{0,0,0} + h.c.$                         | $\Sigma_{bb'}$    | $bc'$  | $6 \times [(1, \mathbf{2})_{1,0,0} + h.c.]$  | 0                 |
| $ab$   | $2 \times [(\mathbf{3}, \bar{\mathbf{2}})_{0,0,0} + h.c.]$ | $\Sigma_{ab}$     |        | $(1, \mathbf{2})_{1,0,0} + h.c.$             | $\Sigma_{bc'}$    |
| $ac$   | $3 \times [(\mathbf{3}, 1)_{-1,0,0} + h.c.]$               | 0                 | $ce$   | $2 \times [(1, 1)_{1,0,-1} + h.c.]$          | $\Sigma_{ce}$     |
|  | $4 \times [(\mathbf{3}, 1)_{-1,0,0} + h.c.]$               | $\Sigma_{ac}$     | $ce'$  | $2 \times [(1, 1)_{1,0,1} + h.c.]$           | $\Sigma_{ce'}$    |
| $ac'$  | $3 \times [(\mathbf{3}, 1)_{1,0,0} + h.c.]$                | 0                 | $de$   | $3 \times [(1, 1)_{0,1,-1} + h.c.]$          | 0                 |
|  | $4 \times [(\mathbf{3}, 1)_{1,0,0} + h.c.]$                | $\Sigma_{ac'}$    |        | $(1, 1)_{0,1,-1} + h.c.$                     | $\Sigma_{de}$     |
| $ad$   | $3 \times [(\mathbf{3}, 1)_{0,-1,0} + h.c.]$               | 0                 | $de'$  | $3 \times [(1, 1)_{0,1,1} + h.c.]$           | 0                 |
|  | $4 \times [(\mathbf{3}, 1)_{0,-1,0} + h.c.]$               | $\Sigma_{ad}$     |        | $(1, 1)_{0,1,1} + h.c.$                      | $\Sigma_{de'}$    |

Table 14: Non-chiral massless and light open spectrum of the model in table 11 on **AAB** computed from 3-cycles. If the factorizable cycles are parallel on  $T_3^2$ , the mass of the states is proportional to the relative distance  $\Sigma_{xy} = |\sigma_{56}^x - \sigma_{56}^y|$  of the D6-branes on this torus,  $\sqrt{\alpha'}m_{xy} = \Sigma_{xy}$ . The distance has to be taken to be in the range  $\Sigma_{xy} \in [0, 1/2] \times R_3$  with  $R_3$  being the (dimensionless) length scale on  $T_3^2$ .  $\sigma_{56}^x$  denotes the distance of brane  $x$  from the origin on  $T_3^2$ . The  $\mathbf{3}_A$  of  $U(3)_a$  transforms as  $\mathbf{3}_2$  under the decomposition  $U(3)_a \rightarrow SU(3)_a \times U(1)_a$ , while the  $\bar{\mathbf{2}}$  of  $U(2)_b$  decomposes into  $\mathbf{2}_{-1}$  of  $SU(2)_b \times U(1)_b$ . The physical  $U(1)$  charges can be computed from section 4.

potential

$$V_D \sim \frac{1}{2g^2} (h_1 \bar{h}_1 - h_2 \bar{h}_2)^2, \quad (50)$$

along which the gauge symmetry is broken to the diagonal subgroup. Here,  $h_1$  and  $h_2$  denote the two chiral multiplets inside the hypermultiplet. If one gauge factor is a  $U(1)$ , there is a potential problem: if the two involved stacks intersect only once (meaning that there is just one hypermultiplet), then the D-flat direction is not F-flat because there is a superpotential, coupling the two chiral multiplets to the adjoint vector multiplet  $\Phi$  as

$$W = h_1 h_2 \Phi. \quad (51)$$

Therefore  $\partial W / \partial \Phi$  imposes  $h_1 h_2 = 0$ , meaning that we cannot give a VEV to both fields  $h_1$  and  $h_2$  at the same time (what D-flatness actually requires).

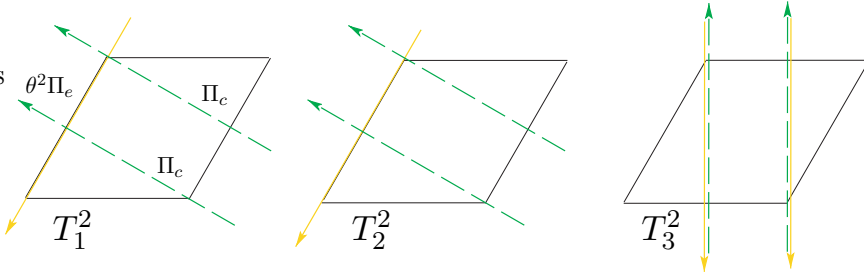


Figure 2: Geometrical intersections of branes  $c$  and  $(\theta^2 e)$  on the **AAB** torus. The gauge group is  $U(1)_c \times U(1)_e$  if the branes are displaced from the origin on  $T_3^2$ . Remember that the  $\mathcal{R}$  invariant plane lies along  $\pi_1 \otimes \pi_3 \otimes (\pi_5 + \pi_6)$  with the notation as in figure 1.

The situation in our case is different: looking at the geometrical intersections of brane  $c$  and  $(\theta^2 e)$  in figure 2, it can be observed that they intersect on both the first and the second torus twice, but hypermultiplets live only on two of intersections, because the relative Wilson line on  $T_1^2$  projects out the other two.

For two hypermultiplets, there is one flat direction which is obtained by combining the VEVs for  $h_1, h_2$  in one hypermultiplet and for  $\tilde{h}_1, \tilde{h}_2$  in the other, such that both the D- and F-flatness conditions are fulfilled. This means explicitly that

$$\begin{aligned} W_1 &= h_1 h_2 \Phi, \\ W_2 &= \tilde{h}_1 \tilde{h}_2 \Phi. \end{aligned} \tag{52}$$

From F-flatness, it is possible to give  $h_2$  and  $\tilde{h}_1$  a non-vanishing VEV (while at the same time giving a vanishing one to  $h_1$  and  $\tilde{h}_2$ ) and still obtain a flat direction in the D-term potential because they couple to the same vectormultiplet  $\Phi$ , i.e. the D-term looks like

$$V_D \sim \frac{1}{2g^2} \left( h_1 \bar{h}_1 - h_2 \bar{h}_2 + \tilde{h}_1 \bar{\tilde{h}}_1 - \tilde{h}_2 \bar{\tilde{h}}_2 \right)^2. \tag{53}$$

The D-term and F-terms are indeed flat for the choice

$$\langle h_1 \rangle = \langle \tilde{h}_2 \rangle = 0, \tag{54}$$

$$\langle h_2 \rangle = \langle \tilde{h}_1 \rangle \neq 0. \tag{55}$$

This construction is just possible if the VEVs that we have given to the fields in between the  $c$  and  $c'$  brane and the  $e$  and  $e'$  brane (formerly the adjoints on the world volume of the  $\Omega\mathcal{R}$  invariant stacks, in order to get  $U(1)$  instead of  $SO(2)$  gauge groups) are the same, but this is completely unproblematic.

Homologically, we only have to add the two cycles  $\Pi_c$  and  $\Pi_e$  to get the recombined brane, which shall be denoted as  $\Pi_C = \Pi_c + \Pi_e$ . This complex cycle has the same volume as the sum of volumes of the two cycles before recombination occurs. The intersection numbers of the recombined cycles are given in table 15. The final chiral spectrum after the recombination is given in table 16. The massless  $U(1)$ s can be checked again using the computation of the Green-Schwarz couplings along the lines of chapter 4. There are two non-anomalous  $U(1)$ s,

| intersections |                |
|---------------|----------------|
| $I_{ab} = 0$  | $I_{ab'} = -3$ |
| $I_{aC} = 3$  | $I_{aC'} = 3$  |
| $I_{bd} = 0$  | $I_{bd'} = 3$  |
| $I_{Cd} = 3$  | $I_{Cd'} = -3$ |
| $I_{bC} = 3$  | $I_{bC'} = 3$  |

Table 15: The intersection numbers (all other intersection numbers vanishing) of the D6-branes in the final 5 stack model on the **AAB** torus.

| Chiral spectrum of 5 stack model on AAB torus |        |   |       |       |       |       |                |
|---|--------|---|-------|-------|-------|-------|----------------|
|   | sector | $SU(3)_a \times SU(2)_b$                  | $Q_a$ | $Q_b$ | $Q_C$ | $Q_d$ | $Q_Y$          |
| $Q_L$   | $ab'$  | $3 \times (\bar{\mathbf{3}}, \mathbf{2})$ | -1    | -1    | 0     | 0     | $\frac{1}{6}$  |
| $U_R$   | $aC$   | $3 \times (\mathbf{3}, 1)$                | 1     | 0     | -1    | 0     | $-\frac{2}{3}$ |
| $D_R$   | $aC'$  | $3 \times (\mathbf{3}, 1)$                | 1     | 0     | 1     | 0     | $\frac{1}{3}$  |
| $L$   | $bd'$  | $3 \times (1, \mathbf{2})$                | 0     | 1     | 0     | 1     | $-\frac{1}{2}$ |
| $E_R$   | $Cd$   | $3 \times (1, 1)$                         | 0     | 0     | 1     | -1    | 1              |
| $N_R$   | $Cd'$  | $3 \times (1, 1)$                         | 0     | 0     | -1    | -1    | 0              |
| $H$   | $bC$   | $3 \times (1, \mathbf{2})$                | 0     | 1     | -1    | 0     | $-\frac{1}{2}$ |
| $\bar{H}$                                     | $bC'$  | $3 \times (1, \mathbf{2})$                | 0     | 1     | 1     | 0     | $\frac{1}{2}$  |

Table 16: Chiral spectrum of the model class with gauge group  $SU(3)_a \times SU(2)_b \times U(1)_a \times U(1)_b \times U(1)_C \times U(1)_d$ .

being  $Q_{B-L} = -\frac{1}{3}Q_a - Q_d$  and  $Q_C$ . Fortunately, the hypercharge

$$Q_Y = -\frac{1}{6}Q_a + \frac{1}{2}Q_C - \frac{1}{2}Q_d \quad (56)$$

is still massless and the two types of fields  $H$  and  $\bar{H}$  have just the opposite hypercharge  $-1/2$  and  $1/2$ . Therefore, they can be exactly understood as the superpartners of the Standard model Higgs with a definite chirality.

## 6.2 The model on the ABA torus

The explicit configuration that shall be discussed in this section is given in table 17, the homological cycles and intersection numbers are listed in table 18.

Comparing table 17 with the model of the preceding section, table 11, reveals that the realization on the torus is very different, for instance in the previous case stacks  $b$  and  $d$  are parallel while in this model stacks  $a$ ,  $b$  and  $d$  are parallel as well as  $c$  and  $e$ . Furthermore, the stacks  $c$  and  $e$  are displaced from the origin on  $T_1^2$ .

|           | $(n_I, m_I)$            | $(\sigma_1, \sigma_2, \sigma_3, \sigma_4)$ | $(\tau_1, \tau_2)$ | $\mathbb{Z}_2$ |
|-----------|-------------------------|--|--------------------|----------------|
| $N_a = 3$ | $(-1, 1; -1, 1; -2, 1)$ | $(0, 0, 0, 0)$                             | $(0, 0)$           | —              |
| $N_b = 2$ | $(-1, 1; -1, 1; -2, 1)$ | $(0, 0, 0, 0)$                             | $(0, 1)$           | —              |
| $N_c = 1$ | $(-1, 0; -1, 1; -1, 2)$ | $(0, \frac{1}{2}, 0, 0)$                   | $(1, 0)$           | —              |
| $N_d = 1$ | $(-1, 1; -1, 1; -2, 1)$ | $(0, 0, 0, 0)$                             | $(0, 0)$           | +              |
| $N_e = 1$ | $(-1, 0; -1, 1; -1, 2)$ | $(0, \frac{1}{2}, 0, 0)$                   | $(1, 1)$           | —              |

Table 17: The setup of the D6-branes in the 5 stack model on the **ABA** torus.

| homology cycles  | intersections |                |
|--|---------------|----------------|
| $\Pi_a = \frac{1}{2}(\rho_1 + \rho_2 - \varepsilon_1 - \varepsilon_2 - \varepsilon_3 - \tilde{\varepsilon}_1 - \tilde{\varepsilon}_2 - \tilde{\varepsilon}_3)$ | $I_{ab} = 0$  | $I_{ab'} = 3$  |
| $\Pi_b = \frac{1}{2}(\rho_1 + \rho_2 - \varepsilon_1 + \varepsilon_2 + \varepsilon_3 - \tilde{\varepsilon}_1 + \tilde{\varepsilon}_2 + \tilde{\varepsilon}_3)$ | $I_{ac} = -3$ | $I_{ac'} = -3$ |
| $\Pi_c = \frac{1}{2}(\rho_1 + \rho_2 + 3\varepsilon_1 + 2\varepsilon_3 + \varepsilon_4 - \tilde{\varepsilon}_3 + \tilde{\varepsilon}_4)$                       | $I_{bd} = 0$  | $I_{bd'} = -3$ |
| $\Pi_d = \frac{1}{2}(\rho_1 + \rho_2 + \varepsilon_1 + \varepsilon_2 + \varepsilon_3 + \tilde{\varepsilon}_1 + \tilde{\varepsilon}_2 + \tilde{\varepsilon}_3)$ | $I_{cd} = -3$ | $I_{cd'} = 3$  |
| $\Pi_e = \frac{1}{2}(\rho_1 + \rho_2 + 3\varepsilon_1 - 2\varepsilon_3 - \varepsilon_4 + \tilde{\varepsilon}_3 - \tilde{\varepsilon}_4)$                       | $I_{be} = -3$ | $I_{be'} = -3$ |

Table 18: The homology cycles and intersection numbers (all other intersection numbers vanishing) of the D6-branes in the 5 stack model on the **ABA** torus.

Nevertheless, the chiral spectrum agrees up to a conjugation with the chiral spectrum of the model on the **AAB** torus, see table 13. The massless  $U(1)$ s after the application of the Green-Schwarz formalism do also completely agree. On the other hand, calculating the non-chiral spectrum for this second explicit model shows that it is indeed very different as compared to the one on the **AAB** torus. The spectrum is listed in table 19. Remarkably, the brane recombination mechanism which has been described in the last section does not work for this model: the hypermultiplets in the sector between the  $c$  and the  $e$  brane are absent due to the relative Wilson line on  $T_2^2$ .

Therefore, we can draw the conclusion that it is only possible for a subclass of models with the same initial chiral spectrum to break it to the exact supersymmetric standard model.

| Non-chiral massless and light open spectrum, <b>ABA</b> on $T^6/(\mathbb{Z}_6 \times \Omega\mathcal{R})$ |  |                     |               |   |                                 |
|--|--|---------------------|---------------|---|---------------------------------|
| sector   | $U(3)_a \times U(2)_b(Q_c, Q_d, Q_e)$  | $\sqrt{\alpha'}m$   | sector        | $U(3)_a \times U(2)_b(Q_c, Q_d, Q_e)$                                 | $\sqrt{\alpha'}m$               |
| $aa$   | $4 \times (\mathbf{9}, 1)_{0,0,0}$   | 0                   | $ab$          | $3 \times [(\mathbf{3}, \bar{\mathbf{2}})_{0,0,0} + h.c.]$            | 0                               |
| $bb$   | $4 \times (\mathbf{1}, \mathbf{4})_{0,0,0}$  | 0                   | $ab'$         | $(\mathbf{3}, \mathbf{2})_{0,0,0} + h.c.$                             | $\Sigma_{ab'}$                  |
| $cc$   | $4 \times (\mathbf{1}, \mathbf{1})_{0,0,0}$  | 0                   | $ac$          | $(\mathbf{3}, 1)_{-1,0,0} + h.c.$                                     | $\Sigma_{ac}$                   |
| $dd$   | $4 \times (\mathbf{1}, \mathbf{1})_{0,0,0}$  | 0                   | $ac'$         | $(\mathbf{3}, 1)_{1,0,0} + h.c.$                                      | $\Sigma_{ac'}$                  |
| $ee$   | $4 \times (\mathbf{1}, \mathbf{1})_{0,0,0}$  | 0                   | $ad$          | $2 \times [(\mathbf{3}, 1)_{0,-1,0} + h.c.]$                          | $\Sigma_{ad}$                   |
| $aa'$  | $(2 \times \mathbf{3}_A + \mathbf{6}_S, 1)_{0,0,0} + h.c.$<br>$(\mathbf{3}_A, 1)_{0,0,0} + h.c.$ | 0<br>$\Sigma_{aa'}$ | $ad'$         | $3 \times [(\mathbf{3}, 1)_{0,1,0} + h.c.]$                           | 0                               |
| $bb'$  | $(1, 2 \times \mathbf{1}_A + \mathbf{3}_S)_{0,0,0} + h.c.$<br>$(1, \mathbf{1}_A)_{0,0,0} + h.c.$ | 0<br>$\Sigma_{bb'}$ | $ae$<br>$ae'$ | $(\mathbf{3}, 1)_{0,0,-1} + h.c.$<br>$(\mathbf{3}, 1)_{0,0,1} + h.c.$ | $\Sigma_{ae}$<br>$\Sigma_{ae'}$ |
| $cc'$  | $(1, 1)_{2,0,0} + h.c.$  | 0                   | $bc$          | $(1, \mathbf{2})_{-1,0,0} + h.c.$                                     | $\Sigma_{bc}$                   |
| $dd'$  | $(1, 1)_{0,2,0} + h.c.$  | 0                   | $bc'$         | $(1, \mathbf{2})_{1,0,0} + h.c.$                                      | $\Sigma_{bc'}$                  |
| $ee'$  | $(1, 1)_{0,0,2} + h.c.$  | 0                   | $be$<br>$be'$ | $(1, \mathbf{2})_{0,0,-1} + h.c.$<br>$(1, \mathbf{2})_{0,0,1} + h.c.$ | $\Sigma_{be}$<br>$\Sigma_{be'}$ |

Table 19: Non-chiral massless and light open spectrum of the model from table 17 on the **ABA** torus. The notation agrees with table 14.

## 7 Left-right symmetric models

In order to obtain a left-right symmetric model with three quark generations, also at least five stacks are required. For the lattices **AAA**, **BBA** and **BBB**, it turns out that all brane configurations with  $SU(3)_a \times SU(2)_b \times SU(2)_c$ , no (anti)symmetric chiral states of  $SU(3)_a$ , i.e.  $\Pi_a \circ \Pi_{a'} = 0$ , and three left and right handed quark generations, i.e.  $3 \times (\mathbf{3}_a, \mathbf{2}_b) + 3 \times (\bar{\mathbf{3}}_a, \mathbf{2}_c)$  in the chiral spectrum, wrap larger bulk cycles than the O6-planes. Therefore, no supersymmetric chiral left-right symmetric 3-generation model on these tori fulfills RR tadpole cancellation. This result agrees completely with the observation made for the ansatz  $N_a = 3$ ,  $N_b = 2$  and  $N_c = 1$  in the previous section. For the **ABA** and **ABB** lattices, the minimal requirement on three stacks of fractional D6-branes can be fulfilled. However, the twisted RR charges cannot be cancelled by any configuration with at most five stacks of D6-branes - at least if we require that the two additional gauge groups have at most rank two.

For the lattice **AAB**, there exist chiral 3-generation left-right symmetric models with five stacks. Two distinct chiral spectra occur, one of them containing (anti)symmetric representations of some  $SU(2)$  factors. The other chiral spectrum encloses only bifundamental representations as displayed in table 20. The gauge group of the standard model part consists of  $SU(3)_a \times SU(2)_b \times SU(2)_c \times U(1)_d$ . In order to fulfill tadpole cancellation, an additional stack with gauge group  $U(2)_e$  is required. Apart from the left/right symmetric MSSM particles, two kinds of exotic chiral particles charged under the additional  $U(2)_e$  arise. These seemingly unwanted exotic particles, however, have the correct quantum numbers to combine into composite Higgs particles. I.e., also in the left/right symmetric models the Higgs fields can originate from

the chiral spectrum due to an ‘internal’  $U(2)_e$  symmetry.

| Chiral left-right symmetric spectrum of an <b>AAB</b> model on $T^6/(\mathbb{Z}_6 \times \Omega\mathcal{R})$ |        |  |       |       |       |       |       |           |             |
|--|--------|--|-------|-------|-------|-------|-------|-----------|-------------|
|  | sector | $SU(3)_a \times SU(2)_b \times SU(2)_c \times SU(2)_e$ | $Q_a$ | $Q_b$ | $Q_c$ | $Q_d$ | $Q_e$ | $Q_{B-L}$ | $\tilde{Q}$ |
| $Q_L$  | $ab'$  | $3 \times (\mathbf{3}, \mathbf{2}, 1; 1)$              | 1     | 1     | 0     | 0     | 0     | $1/3$     | 2           |
| $U_R, D_R$   | $ac'$  | $3 \times (\bar{\mathbf{3}}, 1, \mathbf{2}; 1)$        | -1    | 0     | -1    | 0     | 0     | $-1/3$    | -2          |
| $L$  | $bd'$  | $3 \times (1, \mathbf{2}, 1; 1)$                       | 0     | -1    | 0     | -1    | 0     | -1        | -1          |
| $E_R, N_R$   | $cd'$  | $3 \times (1, 1, \mathbf{2}; 1)$                       | 0     | 0     | 1     | 1     | 0     | 1         | 1           |
|  | $be'$  | $3 \times (1, \mathbf{2}, 1; \mathbf{2})$              | 0     | -1    | 0     | 0     | -1    | 0         | $-5/2$      |
|  | $ce'$  | $3 \times (1, 1, \mathbf{2}; \mathbf{2})$              | 0     | 0     | 1     | 0     | 1     | 0         | $5/2$       |

Table 20: Chiral spectrum of a left-right symmetric model. In the last two columns, the charges under the two massless linear combinations for the specific D6-brane configuration (21) are displayed.

A concrete realisation of this chiral spectrum is given in table 21. The corresponding 3-

|           | $(n_I, m_I)$            | $(\sigma_1, \sigma_2, \sigma_3, \sigma_4)$ | $(\tau_1, \tau_2)$ | $\mathbb{Z}_2 (= \tau_0)$ |
|-----------|-------------------------|--|--------------------|---------------------------|
| $N_a = 3$ | $(-2, 1; -1, 2; -2, 1)$ | $(0, 0, 0, 0)$                             | $(0, 0)$           | -                         |
| $N_b = 2$ | $(-1, 0; -1, 1; -1, 2)$ | $(0, 0, 0, 0)$                             | $(0, 1)$           | +                         |
| $N_c = 2$ | $(-1, 0; -1, 1; -1, 2)$ | $(0, 0, 0, 0)$                             | $(1, 0)$           | +                         |
| $N_d = 1$ | $(-1, 0; -1, 1; -1, 2)$ | $(0, 0, 0, 0)$                             | $(0, 0)$           | -                         |
| $N_e = 2$ | $(-1, 0; -1, 1; -1, 2)$ | $(0, 0, 0, 0)$                             | $(1, 1)$           | +                         |

Table 21: The setup of the D6-branes in the 5 stack left/right symmetric model on the **AAB** torus.

cycles can be read off from tables 23 and 24. Two Abelian gauge factors remain massless,

$$Q_{B-L} = \frac{1}{3}Q_a + Q_d, \quad \tilde{Q} = \frac{1}{4}(3Q_a + 5Q_b + 5Q_c - Q_d + 5Q_e). \quad (57)$$

The non-chiral massless spectrum of the configuration 21 is listed in table 22.

## 8 Conclusions and prospects

In this article, we have worked out all technical details of computing chiral and non-chiral massless spectra for intersecting fractional D6-branes on the  $\mathbb{Z}_6$  orientifold. Discrete Wilson lines and distances of branes naturally occur due to the existence of exceptional cycles. The  $\mathbb{Z}_3$  subsymmetry on each two torus freezes all complex structure moduli. Supersymmetry projects onto one out of two possible toroidal cycles. In addition, the D6-branes can wrap some of the ten existing exceptional 3-cycles. This leads to a  $\mathcal{N} = 2$  supersymmetric gauge sector as compared to the  $\mathcal{N} = 4$  ones for toroidal and orbifold backgrounds without exceptional 3-cycles.

| Non-chiral left-right massless and light open spectrum, AAB, $T^6/(\mathbb{Z}_6 \times \Omega\mathcal{R})$ |  |        |  |
|--|--|--------|--|
| sector   | $U(3)_a \times U(2)_b \times U(2)_c \times U(2)_e (\times U(1)_d)$ | sector | $U(3)_a \times U(2)_b \times U(2)_c \times U(2)_e (\times U(1)_d)$ |
| $aa$   | $16 \times (\mathbf{9}, 1, 1; 1)_0$                                | $ad$   | $7 \times [(\mathbf{3}, 1, 1; 1)_{-1} + h.c.]$                     |
| $bb$   | $4 \times (1, \mathbf{4}, 1; 1)_0$                                 | $ad'$  | $7 \times [(\mathbf{3}, 1, 1; 1)_1 + h.c.]$                        |
| $cc$   | $4 \times (1, 1, \mathbf{4}; 1)_0$                                 | $ae$   | $2 \times [(\mathbf{3}, 1, 1; \bar{\mathbf{2}})_0 + h.c.]$         |
| $dd$   | $4 \times (1, 1, 1; 1)_0$  | $ae'$  | $3 \times [(\mathbf{3}, 1, 1; \mathbf{2})_0 + h.c.]$               |
| $ee$   | $4 \times (1, 1, 1; \mathbf{4})_0$                                 | $bc$   | $3 \times [(1, \mathbf{2}, \bar{\mathbf{2}}; 1)_0 + h.c.]$         |
| $aa'$  | $14 \times [(\mathbf{3}_A, 1, 1; 1)_0 + h.c.]$                     | $bc'$  | $3 \times [(1, \mathbf{2}, \mathbf{2}; 1)_0 + h.c.]$               |
| $bb'$  | $4 \times [(1, \mathbf{1}_A, 1; 1)_0 + h.c.]$                      | $be$   | $3 \times [(1, \mathbf{2}, 1; \bar{\mathbf{2}})_0 + h.c.]$         |
| $cc'$  | $4 \times [(1, 1, \mathbf{1}_A; 1)_0 + h.c.]$                      | $be'$  | $(1, \mathbf{2}, 1; \mathbf{2})_0 + h.c.$                          |
| $ee'$  | $4 \times [(1, 1, 1; \mathbf{1}_A)_0 + h.c.]$                      | $ce$   | $3 \times [(1, 1, \mathbf{2}; \bar{\mathbf{2}})_0 + h.c.]$         |
| $ab$   | $2 \times [(\mathbf{3}, \bar{\mathbf{2}}, 1; 1)_0 + h.c.]$         | $ce'$  | $(1, 1, \mathbf{2}; \mathbf{2})_0 + h.c.$                          |
| $ac$   | $2 \times [(\mathbf{3}, 1, \bar{\mathbf{2}}; 1)_0 + h.c.]$         |        |  |

Table 22: Non-chiral massless and light open spectrum of the left/right symmetric model computed from cycles.

In a supersymmetric set-up, all contributions to the bulk cycles are proportional to those of the O6-planes. In the  $\mathbb{Z}_6$  orientifold, therefore, non-trivial intersections arise purely from the exceptional part of fractional branes. This approach also could be generalized to the two further symmetric orbifold groups  $\mathbb{Z}_6 \times \mathbb{Z}_3$  and  $\mathbb{Z}_{6'}$ . The former is briefly mentioned in appendix D, but does not seem to be of any phenomenological interest due to the small number of fractional cycles.

Already for 2-stack configurations, non-trivial chiral spectra with bifundamental representations exist. By systematically examining the possible 2, 3 and 4-stack configurations, we find that they cannot provide for non-trivial chiral spectra with the Standard model gauge group. In all models, RR tadpoles are cancelled and supersymmetry is preserved globally, ensuring also the absence of NS-NS tadpoles.

The first configurations with the Standard model gauge group and also the correct chiral matter exist for 5 stacks. The most miraculous fact is that with only making the requirements of having at least one 3-, one 2- and one 1-stack of branes, having 3 quark generations, no chiral matter in antisymmetric representations, and preserving globally  $\mathcal{N} = 1$  supersymmetry, there remains only *one* model with a definite chiral spectrum, which is shown in table 13.

Looking more closely at this model, it is not just very aesthetical in having only non-vanishing intersection numbers of an absolute value of 3, beside a massless hypercharge, it also seems to give rise to exactly the standard model particles in the chiral spectrum in addition to two additional kinds of particles in the bifundamental representation  $(1, \mathbf{2})$  of  $U(1) \times U(2)$ . This looks like the two superpartners of the Higgs in a supersymmetric standard model, the only seemingly problem being the fact that the  $U(1)$  is not from the right stack, so at first sight they cannot give rise to the standard Yukawa couplings.

The non-chiral spectrum is rather different for two representants of the discussed class of models. However, through a well motivated brane recombination process which is shown to ex-

actly correspond to a Higgs branch in the effective  $\mathcal{N} = 2$  theory of the type  $U(1) \times U(1) \rightarrow U(1)$ , these particles indeed can be identified with the two kinds of Higgs multiplets in one concrete realization. In homology, this process just means that we add the two factorizable 3-cycles for the two involved  $U(1)$ -branes to get the recombined one, which then is non-factorizable. In the second presented example, the recombination still works in homology, but cannot be understood as a Higgs effect in the effective field theory, because the necessary fields in between the two branes are missing.

We have to emphasize again that the model presented in section 6 therefore represents the first compactification with intersecting branes and genuinely three generations, i.e. no brane recombination is required to obtain three quark and lepton families.

A similar reasoning applies to the left-right symmetric model displayed in section 7.

It will be interesting, to explore the whole class of discussed models with the given chiral spectrum in more detail, meaning that one could compare all different concrete realizations in a spirit like in [72]. Besides, the behavior of the Yukawa and gauge coupling constants depends on the internal geometry and the full massless spectrum. For instance, one could try to calculate the threshold corrections to these models as in [46] and determine if gauge coupling unification is possible [47]. Furthermore, supersymmetry breaking sources should arise at some point and might be understandable in these models. All these tasks hopefully will be achieved in the future [73].

### Acknowledgments

It is a pleasure to thank L. Görlich, K. Landsteiner, A. Uranga, K. Wendland, J. Cascales, W. Troost, A. van Proeyen, D. Lüst and especially R. Blumenhagen and L. Huiszoon for helpful discussions.

This work is supported by the RTN programs under contract numbers HPRN-CT-2000-00131 and HPRN-CT-2000-00148.

## A Basis for a $\mathbb{Z}_3$ invariant 2-torus

We fix the angle between the two basis vectors of a  $\mathbb{Z}_3$  invariant 2-torus to be  $\pi/3$ . With this restriction, the two possible  $\mathcal{R}$  invariant lattices are spanned by

$$\begin{aligned} e_1^{\mathbf{A}} &= \begin{pmatrix} \sqrt{2} \\ 0 \end{pmatrix}, & e_2^{\mathbf{A}} &= \begin{pmatrix} 1/\sqrt{2} \\ \sqrt{3/2} \end{pmatrix}, \\ e_1^{*\mathbf{A}} &= \begin{pmatrix} 1/\sqrt{2} \\ -1/\sqrt{6} \end{pmatrix}, & e_2^{*\mathbf{A}} &= \begin{pmatrix} 0 \\ \sqrt{2/3} \end{pmatrix}, \end{aligned} \tag{58}$$

for the **A** orientation where  $\pi_{2k-1}$  lies on the  $\mathcal{R}$  invariant plane, and

$$\begin{aligned} e_1^{\mathbf{B}} &= \begin{pmatrix} \sqrt{3/2} \\ -1/\sqrt{2} \end{pmatrix}, & e_2^{\mathbf{B}} &= \begin{pmatrix} \sqrt{3/2} \\ 1/\sqrt{2} \end{pmatrix}, \\ e_1^{*\mathbf{B}} &= \begin{pmatrix} 1/\sqrt{6} \\ -1/\sqrt{2} \end{pmatrix}, & e_2^{*\mathbf{B}} &= \begin{pmatrix} 1/\sqrt{6} \\ 1/\sqrt{2} \end{pmatrix}, \end{aligned} \tag{59}$$

for the **B** orientation where  $\mathcal{R}$  exchanges  $\pi_{2k-1}$  and  $\pi_{2k}$ .

## B Exceptional cycles, wrapping numbers and fixed points on $T_1^2 \times T_2^2$

| Wrapping numbers intersecting fixed points for $T^6/\mathbb{Z}_6$ |                                 |                                 |                                 |  |                                 |                                 |
|---|---------------------------------|---------------------------------|---------------------------------|--|---------------------------------|---------------------------------|
| $(n_2, m_2)$  | (odd, even)                     | (even, odd)                     | (odd, odd)                      | (odd, even)                            | (even, odd)                     | (odd, odd)                      |
| $(n_1, m_1)$  | $\sigma_3 = \sigma_4 = 0$       |                                 |                                 | $\sigma_3 = \frac{1}{2}, \sigma_4 = 0$ |                                 |                                 |
| $\sigma_1 = \sigma_2 = 0$   |                                 |                                 |                                 |  |                                 |                                 |
| (odd, even)   | $(e_{11}) e_{14} e_{41} e_{44}$ | $(e_{11}) e_{15} e_{41} e_{45}$ | $(e_{11}) e_{16} e_{41} e_{46}$ | $(e_{11}) e_{14} e_{41} e_{44}$        | $e_{14} e_{16} e_{44} e_{46}$   | $e_{14} e_{15} e_{44} e_{45}$   |
| (even, odd)   | $(e_{11}) e_{14} e_{51} e_{54}$ | $(e_{11}) e_{15} e_{51} e_{55}$ | $(e_{11}) e_{16} e_{51} e_{56}$ | $(e_{11}) e_{14} e_{51} e_{54}$        | $e_{14} e_{16} e_{54} e_{56}$   | $e_{14} e_{15} e_{54} e_{55}$   |
| (odd, odd)  | $(e_{11}) e_{14} e_{61} e_{64}$ | $(e_{11}) e_{15} e_{61} e_{65}$ | $(e_{11}) e_{16} e_{61} e_{66}$ | $(e_{11}) e_{14} e_{61} e_{64}$        | $e_{14} e_{16} e_{64} e_{66}$   | $e_{14} e_{15} e_{64} e_{65}$   |
| $\sigma_1 = \frac{1}{2}, \sigma_2 = 0$                            |                                 |                                 |                                 |  |                                 |                                 |
| (odd, even)   | $(e_{11}) e_{14} e_{41} e_{44}$ | $(e_{11}) e_{15} e_{41} e_{45}$ | $(e_{11}) e_{16} e_{41} e_{46}$ | $(e_{11}) e_{14} e_{41} e_{44}$        | $e_{14} e_{16} e_{44} e_{46}$   | $e_{14} e_{15} e_{44} e_{45}$   |
| (even, odd)   | $e_{61} e_{64} e_{41} e_{44}$   | $e_{61} e_{65} e_{41} e_{45}$   | $e_{61} e_{66} e_{41} e_{46}$   | $e_{61} e_{64} e_{41} e_{44}$          | $e_{64} e_{66} e_{44} e_{46}$   | $e_{64} e_{65} e_{44} e_{45}$   |
| (odd, odd)  | $e_{51} e_{54} e_{41} e_{44}$   | $e_{51} e_{55} e_{41} e_{45}$   | $e_{51} e_{56} e_{41} e_{46}$   | $e_{51} e_{54} e_{41} e_{44}$          | $e_{54} e_{56} e_{44} e_{46}$   | $e_{54} e_{55} e_{44} e_{45}$   |
| $\sigma_1 = 0, \sigma_2 = \frac{1}{2}$                            |                                 |                                 |                                 |  |                                 |                                 |
| (odd, even)   | $e_{61} e_{64} e_{51} e_{54}$   | $e_{61} e_{65} e_{51} e_{55}$   | $e_{61} e_{66} e_{51} e_{56}$   | $e_{61} e_{64} e_{51} e_{54}$          | $e_{64} e_{66} e_{54} e_{56}$   | $e_{64} e_{65} e_{54} e_{55}$   |
| (even, odd)   | $(e_{11}) e_{14} e_{51} e_{54}$ | $(e_{11}) e_{15} e_{51} e_{55}$ | $(e_{11}) e_{16} e_{51} e_{56}$ | $(e_{11}) e_{14} e_{51} e_{54}$        | $e_{14} e_{16} e_{54} e_{56}$   | $e_{14} e_{15} e_{54} e_{55}$   |
| (odd, odd)  | $e_{41} e_{44} e_{51} e_{54}$   | $e_{41} e_{45} e_{51} e_{55}$   | $e_{41} e_{46} e_{51} e_{56}$   | $e_{41} e_{44} e_{51} e_{54}$          | $e_{44} e_{46} e_{54} e_{56}$   | $e_{44} e_{45} e_{54} e_{55}$   |
| $\sigma_1 = \sigma_2 = \frac{1}{2}$                               |                                 |                                 |                                 |  |                                 |                                 |
| (odd, even)   | $e_{61} e_{64} e_{51} e_{54}$   | $e_{61} e_{65} e_{51} e_{55}$   | $e_{61} e_{66} e_{51} e_{56}$   | $e_{61} e_{64} e_{51} e_{54}$          | $e_{64} e_{66} e_{54} e_{56}$   | $e_{64} e_{65} e_{54} e_{55}$   |
| (even, odd)   | $e_{41} e_{44} e_{61} e_{64}$   | $e_{41} e_{45} e_{61} e_{65}$   | $e_{41} e_{46} e_{61} e_{66}$   | $e_{41} e_{44} e_{61} e_{64}$          | $e_{44} e_{46} e_{64} e_{66}$   | $e_{44} e_{45} e_{64} e_{65}$   |
| (odd, odd)  | $(e_{11}) e_{14} e_{61} e_{64}$ | $(e_{11}) e_{15} e_{61} e_{65}$ | $(e_{11}) e_{16} e_{61} e_{66}$ | $(e_{11}) e_{14} e_{61} e_{64}$        | $e_{14} e_{16} e_{64} e_{66}$   | $e_{14} e_{15} e_{64} e_{65}$   |
| $\sigma_3 = 0, \sigma_4 = \frac{1}{2}$                            |                                 |                                 |                                 |  |                                 |                                 |
| $\sigma_1 = \sigma_2 = 0$   |                                 |                                 |                                 |  |                                 |                                 |
| (odd, even)   | $e_{15} e_{16} e_{45} e_{46}$   | $(e_{11}) e_{15} e_{41} e_{45}$ | $e_{15} e_{14} e_{44} e_{45}$   | $e_{15} e_{16} e_{45} e_{46}$          | $e_{14} e_{16} e_{44} e_{46}$   | $(e_{11}) e_{16} e_{41} e_{46}$ |
| (even, odd)   | $e_{15} e_{16} e_{55} e_{56}$   | $(e_{11}) e_{15} e_{51} e_{55}$ | $e_{14} e_{15} e_{54} e_{55}$   | $e_{15} e_{16} e_{55} e_{56}$          | $e_{14} e_{16} e_{54} e_{56}$   | $(e_{11}) e_{16} e_{51} e_{56}$ |
| (odd, odd)  | $e_{15} e_{16} e_{65} e_{66}$   | $(e_{11}) e_{15} e_{61} e_{65}$ | $e_{14} e_{15} e_{64} e_{65}$   | $e_{15} e_{16} e_{65} e_{66}$          | $e_{14} e_{16} e_{64} e_{66}$   | $(e_{11}) e_{16} e_{61} e_{66}$ |
| $\sigma_1 = \frac{1}{2}, \sigma_2 = 0$                            |                                 |                                 |                                 |  |                                 |                                 |
| (odd, even)   | $e_{15} e_{16} e_{45} e_{46}$   | $(e_{11}) e_{15} e_{41} e_{45}$ | $e_{14} e_{15} e_{44} e_{45}$   | $e_{15} e_{16} e_{45} e_{46}$          | $e_{14} e_{16} e_{44} e_{46}$   | $(e_{11}) e_{16} e_{41} e_{46}$ |
| (even, odd)   | $e_{65} e_{66} e_{45} e_{46}$   | $e_{61} e_{65} e_{41} e_{45}$   | $e_{64} e_{65} e_{44} e_{45}$   | $e_{65} e_{66} e_{45} e_{46}$          | $e_{64} e_{66} e_{44} e_{46}$   | $e_{61} e_{66} e_{41} e_{46}$   |
| (odd, odd)  | $e_{55} e_{56} e_{45} e_{46}$   | $e_{51} e_{55} e_{41} e_{45}$   | $e_{54} e_{55} e_{44} e_{45}$   | $e_{55} e_{56} e_{45} e_{46}$          | $e_{54} e_{56} e_{44} e_{46}$   | $e_{51} e_{56} e_{41} e_{46}$   |
| $\sigma_1 = 0, \sigma_2 = \frac{1}{2}$                            |                                 |                                 |                                 |  |                                 |                                 |
| (odd, even)   | $e_{65} e_{66} e_{55} e_{56}$   | $e_{61} e_{65} e_{51} e_{55}$   | $e_{64} e_{65} e_{54} e_{55}$   | $e_{65} e_{66} e_{55} e_{56}$          | $e_{64} e_{66} e_{54} e_{56}$   | $e_{61} e_{66} e_{51} e_{56}$   |
| (even, odd)   | $(e_{11}) e_{15} e_{51} e_{55}$ | $e_{14} e_{15} e_{54} e_{55}$   | $e_{15} e_{16} e_{55} e_{56}$   | $e_{14} e_{16} e_{54} e_{56}$          | $(e_{11}) e_{16} e_{51} e_{56}$ |                                 |
| (odd, odd)  | $e_{45} e_{46} e_{55} e_{56}$   | $e_{41} e_{45} e_{51} e_{55}$   | $e_{44} e_{45} e_{54} e_{55}$   | $e_{45} e_{46} e_{55} e_{56}$          | $e_{44} e_{46} e_{54} e_{56}$   | $e_{41} e_{46} e_{51} e_{56}$   |
| $\sigma_1 = \sigma_2 = \frac{1}{2}$                               |                                 |                                 |                                 |  |                                 |                                 |
| (odd, even)   | $e_{65} e_{66} e_{55} e_{56}$   | $e_{61} e_{65} e_{51} e_{55}$   | $e_{64} e_{65} e_{54} e_{55}$   | $e_{65} e_{66} e_{55} e_{56}$          | $e_{64} e_{66} e_{54} e_{56}$   | $e_{61} e_{66} e_{51} e_{56}$   |
| (even, odd)   | $e_{45} e_{46} e_{65} e_{66}$   | $e_{41} e_{45} e_{61} e_{65}$   | $e_{44} e_{45} e_{64} e_{65}$   | $e_{45} e_{46} e_{65} e_{66}$          | $e_{44} e_{46} e_{64} e_{66}$   | $e_{41} e_{46} e_{61} e_{66}$   |
| (odd, odd)  | $(e_{11}) e_{16} e_{65} e_{66}$ | $(e_{11}) e_{15} e_{61} e_{65}$ | $e_{14} e_{15} e_{64} e_{65}$   | $e_{15} e_{16} e_{65} e_{66}$          | $e_{14} e_{16} e_{64} e_{66}$   | $(e_{11}) e_{16} e_{61} e_{66}$ |

Table 23: Relation between fixed points and wrapping numbers on  $T_1^2 \times T_2^2$ . The fixed point  $e_{11}$  does not give rise to any exceptional cycle. The bulk 2-cycle specified by the wrapping numbers can be displaced from the origin by  $\sum_{i=1}^4 \sigma_i \pi_i$  with  $\sigma_i \in \{0, 1/2\}$ .

| 2-cycle $\otimes$ 1-cycle              | Exceptional 3-cycle  |
|--|--|
| $e_{11} \otimes (n_3\pi_5 + m_3\pi_6)$ | ---  |
| $e_{14} \otimes (n_3\pi_5 + m_3\pi_6)$ | $n_3\varepsilon_2 + m_3\tilde{\varepsilon}_2$                            |
| $e_{15} \otimes (n_3\pi_5 + m_3\pi_6)$ | $n_3(\tilde{\varepsilon}_2 - \varepsilon_2) - m_3\varepsilon_2$          |
| $e_{16} \otimes (n_3\pi_5 + m_3\pi_6)$ | $-n_3\tilde{\varepsilon}_2 - m_3(\tilde{\varepsilon}_2 - \varepsilon_2)$ |
| $e_{41} \otimes (n_3\pi_5 + m_3\pi_6)$ | $n_3\varepsilon_1 + m_3\tilde{\varepsilon}_1$                            |
| $e_{51} \otimes (n_3\pi_5 + m_3\pi_6)$ | $n_3(\tilde{\varepsilon}_1 - \varepsilon_1) - m_3\varepsilon_1$          |
| $e_{61} \otimes (n_3\pi_5 + m_3\pi_6)$ | $-n_3\tilde{\varepsilon}_1 - m_3(\tilde{\varepsilon}_1 - \varepsilon_1)$ |
| $e_{44} \otimes (n_3\pi_5 + m_3\pi_6)$ | $n_3\varepsilon_3 + m_3\tilde{\varepsilon}_3$                            |
| $e_{45} \otimes (n_3\pi_5 + m_3\pi_6)$ | $n_3\varepsilon_4 + m_3\tilde{\varepsilon}_4$                            |
| $e_{46} \otimes (n_3\pi_5 + m_3\pi_6)$ | $n_3\varepsilon_5 + m_3\tilde{\varepsilon}_5$                            |
| $e_{54} \otimes (n_3\pi_5 + m_3\pi_6)$ | $n_3(\tilde{\varepsilon}_5 - \varepsilon_5) - m_3\varepsilon_5$          |
| $e_{55} \otimes (n_3\pi_5 + m_3\pi_6)$ | $n_3(\tilde{\varepsilon}_3 - \varepsilon_3) - m_3\varepsilon_3$          |
| $e_{56} \otimes (n_3\pi_5 + m_3\pi_6)$ | $n_3(\tilde{\varepsilon}_4 - \varepsilon_4) - m_3\varepsilon_4$          |
| $e_{64} \otimes (n_3\pi_5 + m_3\pi_6)$ | $-n_3\tilde{\varepsilon}_4 - m_3(\tilde{\varepsilon}_4 - \varepsilon_4)$ |
| $e_{65} \otimes (n_3\pi_5 + m_3\pi_6)$ | $-n_3\tilde{\varepsilon}_5 - m_3(\tilde{\varepsilon}_5 - \varepsilon_5)$ |
| $e_{66} \otimes (n_3\pi_5 + m_3\pi_6)$ | $-n_3\tilde{\varepsilon}_3 - m_3(\tilde{\varepsilon}_3 - \varepsilon_3)$ |

Table 24: Relation between orbits of fixed points and cycles as read off from (13).

## C Some loop an tree channel results

### C.1 Tree channel bulk part

The oscillator expansion of an untwisted boundary state (30) with spin structure  $\eta = \pm 1$  and relative angles  $\pi\varphi_a^k$  w.r.t.  $\pi_{2k-1}$  is given by [5, 11]

$$|D6; (n_i^a, m_i^a), \eta\rangle \sim \exp \left\{ - \sum_{k=0}^3 \sum_n \frac{e^{2\pi i \varphi_a^k}}{n} \alpha_{-n}^k \tilde{\alpha}_{-n}^k - i\eta \sum_{k=0}^3 \sum_r e^{2\pi i \varphi_a^k} \psi_{-r}^k \tilde{\psi}_{-r}^k + h.c. \right\} |0, \eta; p^k, w^k; \tau_i, \sigma_i\rangle. \quad (60)$$

In order to shorten the notation, the non-compact coordinates are denoted by  $k = 0$  and the corresponding angle is  $\varphi_a^0 \equiv 0$ .

In addition to the Kaluza Klein momenta and windings existing in toroidal compactifications, for fractional branes discrete Wilson lines on  $T_1^2 \times T_2^2$  parameterized by  $\tau_1, \tau_2$  arise from the  $\mathbb{Z}_2$  fixed points [36], see eq. (28). A bulk brane can be displaced from the origin by  $\sum_{i=1}^6 \sigma_i \pi_i$ , with arbitrary values  $\sigma_i \in [0, 1]$ , whereas for a fractional brane the displacement is discretized on two tori,  $\sigma_i \in \{0, 1/2\}$  for  $i = 1, \dots, 4$ .

Relative Wilson lines between two different boundary states which are parallel on a 2-torus give rise to complex phases at each mass level, i.e. if  $L$  is the dimensionless length of the

1-cycle wrapped by the two branes,  $R^2$  the volume of the corresponding 2-torus,  $\frac{\tau}{2} \in \{0, 1/2\}$  the relative Wilson line and  $\sigma$  the spatial separation, the tree channel zero mode contributions are given by

$$\tilde{\mathcal{L}}(l) = \left( \sum_{r \in \mathbb{Z}} e^{-\pi lr^2 L^2 R^2 / \alpha' + \pi i r \tau} \right) \left( \sum_{s \in \mathbb{Z}} e^{-\pi ls^2 L^2 \alpha' / R^4 + 2\pi i s \sigma} \right). \quad (61)$$

Modular transformation leads to the loop channel annulus contribution

$$\mathcal{L}(t) = \left( \sum_{r \in \mathbb{Z}} e^{-2\pi t(r - \tau/2)^2 \alpha' / (R^2 L^2)} \right) \left( \sum_{s \in \mathbb{Z}} e^{-2\pi t(s - \sigma)^2 R^4 / (L^2 \alpha')} \right), \quad (62)$$

which confirms that strings stretching between branes with relative Wilson lines and/or spatial separation do not carry massless modes.

## C.2 Tree channel twisted part

The oscillator modding of a twisted boundary state (31) is shifted by the twist vector  $v = (1/2, -1/2, 0)$ ,

$$\begin{aligned} |D6; (n_3^a, m_3^a), e_{ij}\eta\rangle \sim & \exp \left\{ - \sum_{k=0,3} \sum_n \frac{e^{2\pi i \varphi_a^k}}{n} \alpha_{-n}^k \tilde{\alpha}_{-n}^k - i\eta \sum_{k=0,3} \sum_r e^{2\pi i \varphi_a^k} \psi_{-r}^k \tilde{\psi}_{-r}^k \right. \\ & \left. - \sum_{j=1,2} \sum_n \frac{e^{2\pi i \varphi_a^j}}{n} \alpha_{-n+v_j}^j \tilde{\alpha}_{-n+v_j}^j - i\eta \sum_{j=1,2} \sum_r e^{2\pi i \varphi_a^j} \psi_{-r+v_j}^j \tilde{\psi}_{-r+v_j}^j + h.c. \right\} |0, \eta; p^3, w^3, e_{ij}\rangle, \end{aligned} \quad (63)$$

and the discrete Wilson lines enter the boundary states only as relative signs  $\alpha_{ij}$  between the twisted sector contributions, compare eq. (31).

The crosscap states do not have any twisted contributions.

## C.3 Oscillator contributions to the amplitudes

The tree channel oscillator contributions to the annulus and Möbius strip amplitude are of the form

$$\begin{aligned} \tilde{\mathcal{A}}_{v,(\varphi_1, \varphi_2, \varphi_3)}^{\alpha\beta} &= \frac{\vartheta \begin{bmatrix} \alpha \\ \beta \end{bmatrix}}{\eta^3} \prod_{i=1}^3 \frac{\vartheta \begin{bmatrix} \alpha - v_i \\ \varphi_i + \beta \end{bmatrix}}{\vartheta \begin{bmatrix} 1/2 - v_i \\ \varphi_i + 1/2 \end{bmatrix}} (2l) \\ \tilde{\mathcal{M}}_{(\varphi_1, \varphi_2, \varphi_3)}^{\alpha\beta} &= \frac{\vartheta \begin{bmatrix} \alpha \\ \beta \end{bmatrix}}{\eta^3} \prod_{i=1}^3 \frac{\vartheta \begin{bmatrix} \alpha \\ \varphi_i + \beta \end{bmatrix}}{\vartheta \begin{bmatrix} 1/2 \\ \varphi_i + 1/2 \end{bmatrix}} (2l - i/2) \end{aligned} \quad (64)$$

where  $v = 0$  for the untwisted and  $v = (1/2, -1/2, 0)$  for the  $\mathbb{Z}_2$  twisted annulus contributions.  $\alpha = 0, 1/2$  corresponds to NSNS and RR contributions, respectively and  $\beta = 0, 1/2$  labels

contributions from identical and opposite spin structures. For more details on the notation see e.g. the appendices of [4, 10].

For each vanishing angle  $\varphi_i = 0$  and vanishing twist  $v_i$ , the corresponding denominator has to be replaced,  $\vartheta \begin{bmatrix} 1/2 \\ \varphi_i + 1/2 \end{bmatrix} \xrightarrow{\varphi_i \rightarrow 0} \eta^3$ .

The loop channel oscillator contributions are given by

$$\begin{aligned} \mathcal{A}_{v,(\varphi_1,\varphi_2,\varphi_3)}^{A,B} &= i \frac{\vartheta \begin{bmatrix} A \\ B \end{bmatrix}}{\eta^3} \prod_{i=1}^3 \frac{\vartheta \begin{bmatrix} A - \varphi_i \\ B - v_i \end{bmatrix}}{\vartheta \begin{bmatrix} 1/2 - \varphi_i \\ 1/2 - v_i \end{bmatrix}}(t) \\ \mathcal{M}_{(\varphi_1,\varphi_2,\varphi_3)}^{A,B} &= i \frac{\vartheta \begin{bmatrix} A \\ B \end{bmatrix}}{\eta^3} \prod_{i=1}^3 \frac{\vartheta \begin{bmatrix} A + 2\varphi_i \\ B - \varphi_i \end{bmatrix}}{\vartheta \begin{bmatrix} 1/2 + 2\varphi_i \\ 1/2 - \varphi_i \end{bmatrix}}(t - i/2) \end{aligned} \quad (65)$$

where  $v = 0$  corresponds to an open string state without and  $v = (1/2, -1/2, 0)$  with  $\mathbb{Z}_2$  insertion. The modification for vanishing angle is identical to the tree channel result up to a factor of  $i$ .

The modular transformation for three non-vanishing angles is given by

$$\begin{aligned} \tilde{\mathcal{A}}_{v,(\varphi_1,\varphi_2,\varphi_3)}^{\alpha\beta} &= \frac{e^{\pi i(2\alpha-1)\sum_{i=1}^3 \varphi_i}}{t} \mathcal{A}_{v,(\varphi_1,\varphi_2,\varphi_3)}^{\beta,\alpha}, \\ \tilde{\mathcal{M}}_{(\varphi_1,\varphi_2,\varphi_3)}^{\alpha\beta} &= \frac{e^{2\pi i\alpha}}{2} \frac{e^{4(\alpha+\beta)\pi i \sum_{i=1}^3 \varphi_i}}{t} \mathcal{M}_{(\varphi_1,\varphi_2,\varphi_3)}^{\alpha,1/2-(\alpha+\beta)}. \end{aligned} \quad (66)$$

Each vanishing angle modifies these equations by a factor of  $1/t$  for the annulus and  $1/(2t)$  for the Möbius strip.

## D Some results for $T^6/(\mathbb{Z}_6 \times \mathbb{Z}_3)$

The orbifold generators  $\Theta$  and  $\omega$  are represented by the two shift vectors  $v = (1/6, -1/6, 0)$  and  $w = (0, 1/3, -1/3)$ , respectively. The Hodge numbers are given by (see e.g. [74] and also [10] for the closed string spectrum)

$$\begin{aligned} h_{1,1}^U &= 3, & h_{1,1}^{\theta^3} &= 4, & h_{1,1}^{fixplanes-not-\mathbb{Z}_2} &= 36, & h_{1,1}^{fixpoints} &= 30, \\ h_{2,1}^U &= 0, & h_{2,1}^{\theta^3} &= 1, & h_{2,1}^{fixplanes-not-\mathbb{Z}_2} &= 0, & h_{2,1}^{fixpoints} &= 0. \end{aligned} \quad (67)$$

The allowed compactification lattices are as depicted in figure 1, and the fundamental bulk 3-cycles can be chosen to be identical (up to normalization) to those displayed in eq. (3).

The orbits of wrapping numbers which describe all possible factorizable 3-cycles are given by

$$\begin{aligned}
& \begin{pmatrix} n_1 & m_1 \\ n_2 & m_2 \\ n_3 & m_3 \end{pmatrix} \xrightarrow{\Theta} \begin{pmatrix} -m_1 & n_1 + m_1 \\ (n_2 + m_2) & -n_2 \\ n_3 & m_3 \end{pmatrix} \xrightarrow{\Theta} \begin{pmatrix} -(n_1 + m_1) & n_1 \\ m_2 & -(n_2 + m_2) \\ n_3 & m_3 \end{pmatrix} \\
& \downarrow \omega \\
& \begin{pmatrix} n_1 & m_1 \\ -(n_2 + m_2) & n_2 \\ m_3 & -(n_3 + m_3) \end{pmatrix} \xrightarrow{\Theta} \begin{pmatrix} -m_1 & n_1 + m_1 \\ -m_2 & (n_2 + m_2) \\ m_3 & -(n_3 + m_3) \end{pmatrix} \xrightarrow{\Theta} \begin{pmatrix} -(n_1 + m_1) & n_1 \\ n_2 & m_2 \\ m_3 & -(n_3 + m_3) \end{pmatrix} \\
& \downarrow \omega \\
& \begin{pmatrix} n_1 & m_1 \\ m_2 & -(n_2 + m_2) \\ -(n_3 + m_3) & n_3 \end{pmatrix} \xrightarrow{\Theta} \begin{pmatrix} -m_1 & n_1 + m_1 \\ -n_2 & -m_2 \\ -(n_3 + m_3) & n_3 \end{pmatrix} \xrightarrow{\Theta} \begin{pmatrix} -(n_1 + m_1) & n_1 \\ -(n_2 + m_2) & n_2 \\ -(n_3 + m_3) & n_3 \end{pmatrix}
\end{aligned} \tag{68}$$

and lead (up to normalization) to the coefficients (6) computed for the  $T^6/\mathbb{Z}_6$  case.

Only two exceptional 3-cycles arise. The fixed points on  $T_1^2$  are permuted under  $\Theta$  as in (10) and are fixed under  $\omega$ . On  $T_2^2$ , the permutations are given by

$$\Theta(4) = \omega(4) = 6, \quad \Theta(5) = \omega(5) = 4, \quad \Theta(6) = \omega(6) = 5. \tag{69}$$

On  $T_3^2$ , only  $\omega$  fixed points occur, which transform trivially under  $\Theta$  and do not contribute to exceptional 3-cycles. Two linearly independent, orbifold invariant exceptional 3-cycles with vanishing self-intersection can be expressed in terms of (13),

$$\begin{aligned}
\zeta_1 &= (1 + \Theta + \Theta^2)(1 + \omega + \omega^2)e_{44} \otimes \pi_5 \\
&\sim \varepsilon_3 - \varepsilon_4 + \tilde{\varepsilon}_4 - \tilde{\varepsilon}_5, \\
\zeta_2 &= (1 + \Theta + \Theta^2)(1 + \omega + \omega^2)e_{55} \otimes \pi_5 \\
&\sim -\varepsilon_3 + \varepsilon_5 + \tilde{\varepsilon}_3 - \tilde{\varepsilon}_4.
\end{aligned} \tag{70}$$

## References

- [1] M. Berkooz, M. R. Douglas, and R. G. Leigh. *Branes Intersecting at Angles*. Nucl. Phys. B 480, 265 (1996), [hep-th/9606139](#).
- [2] Augusto Sagnotti. *Open strings and their symmetry groups*. (1987), [hep-th/0208020](#).
- [3] Ralph Blumenhagen, Lars Görlich, and Boris Körs. *A new class of supersymmetric orientifolds with D-branes at angles*. (1999), [hep-th/0002146](#).
- [4] Ralph Blumenhagen, Lars Görlich, and Boris Körs. *Supersymmetric 4D orientifolds of type IIA with D6-branes at angles*. JHEP 01, 040 (2000), [hep-th/9912204](#).
- [5] Ralph Blumenhagen, Lars Görlich, Boris Körs, and Dieter Lüst. *Noncommutative compactifications of type I strings on tori with magnetic background flux*. JHEP 10, 006 (2000), [hep-th/0007024](#).

- [6] Ralph Blumenhagen, Boris Körs, and Dieter Lüst. *Type I strings with F- and B-flux*. JHEP 02, 030 (2001), [hep-th/0012156](#).
- [7] C. Angelantonj, Ignatios Antoniadis, E. Dudas, and A. Sagnotti. *Type-I strings on magnetised orbifolds and brane transmutation*. Phys. Lett. B489, 223–232 (2000), [hep-th/0007090](#).
- [8] G. Aldazabal, S. Franco, Luis E. Ibanez, R. Rabadan, and A. M. Uranga. *Intersecting brane worlds*. JHEP 02, 047 (2001), [hep-ph/0011132](#).
- [9] G. Aldazabal, S. Franco, Luis E. Ibanez, R. Rabadan, and A. M. Uranga.  *$D = 4$  chiral string compactifications from intersecting branes*. J. Math. Phys. 42, 3103–3126 (2001), [hep-th/0011073](#).
- [10] Stefan Forste, Gabriele Honecker, and Ralph Schreyer. *Supersymmetric  $Z(N) \times Z(M)$  orientifolds in 4D with D-branes at angles*. Nucl. Phys. B593, 127–154 (2001), [hep-th/0008250](#).
- [11] Stefan Forste, Gabriele Honecker, and Ralph Schreyer. *Orientifolds with branes at angles*. JHEP 06, 004 (2001), [hep-th/0105208](#).
- [12] Shamit Kachru and John McGreevy. *Supersymmetric three-cycles and (super)symmetry breaking*. Phys. Rev. D61, 026001 (2000), [hep-th/9908135](#).
- [13] Angel M. Uranga. *Chiral four-dimensional string compactifications with intersecting D-branes*. Class. Quant. Grav. 20, S373–S394 (2003), [hep-th/0301032](#).
- [14] Tassilo Ott. *Aspects of stability and phenomenology in type IIA orientifolds with intersecting D6-branes*. (2003), [hep-th/0309107](#).
- [15] Fernando G. Marchesano Buznego. *Intersecting D-brane models*. (2003), [hep-th/0307252](#).
- [16] Lars Görlich.  *$N = 1$  and non-supersymmetric open string theories in six and four space-time dimensions*. (2004), [hep-th/0401040](#).
- [17] Carlo Angelantonj and Augusto Sagnotti. *Open strings*. Phys. Rept. 371, 1–150 (2002), [hep-th/0204089](#).
- [18] Ralph Blumenhagen, Volker Braun, Boris Körs, and Dieter Lüst. *Orientifolds of K3 and Calabi-Yau manifolds with intersecting D-branes*. JHEP 07, 026 (2002), [hep-th/0206038](#).
- [19] Ralph Blumenhagen, Volker Braun, Boris Körs, and Dieter Lüst. *The standard model on the quintic*. (2002), [hep-th/0210083](#).
- [20] Luis E. Ibanez, F. Marchesano, and R. Rabadan. *Getting just the standard model at intersecting branes*. JHEP 11, 002 (2001), [hep-th/0105155](#).
- [21] Christos Kokorelis. *GUT model hierarchies from intersecting branes*. JHEP 08, 018 (2002), [hep-th/0203187](#).
- [22] Christos Kokorelis. *New standard model vacua from intersecting branes*. JHEP 09, 029 (2002), [hep-th/0205147](#).

- [23] Ralph Blumenhagen, Boris Körs, Dieter Lüst, and Tassilo Ott. *The standard model from stable intersecting brane world orbifolds*. Nucl. Phys. B616, 3–33 (2001), [hep-th/0107138](#).
- [24] Ralph Blumenhagen, Boris Körs, Dieter Lüst, and Tassilo Ott. *Intersecting brane worlds on tori and orbifolds*. Fortsch. Phys. 50, 843–850 (2002), [hep-th/0112015](#).
- [25] R. Rabadan. *Branes at angles, torons, stability and supersymmetry*. Nucl. Phys. B620, 152–180 (2002), [hep-th/0107036](#).
- [26] Ralph Blumenhagen, Boris Körs, Dieter Lüst, and Tassilo Ott. *Hybrid inflation in intersecting brane worlds*. Nucl. Phys. B641, 235–255 (2002), [hep-th/0202124](#).
- [27] Juan Garcia-Bellido, Raul Rabadan, and Frederic Zamora. *Inflationary scenarios from branes at angles*. JHEP 01, 036 (2002), [hep-th/0112147](#).
- [28] Mirjam Cvetic, Gary Shiu, and Angel M. Uranga. *Three-family supersymmetric standard like models from intersecting brane worlds*. Phys. Rev. Lett. 87, 201801 (2001), [hep-th/0107143](#).
- [29] Mirjam Cvetic, Gary Shiu, and Angel M. Uranga. *Chiral four-dimensional  $N = 1$  supersymmetric type IIA orientifolds from intersecting D6-branes*. Nucl. Phys. B615, 3–32 (2001), [hep-th/0107166](#).
- [30] Mirjam Cvetic, Paul Langacker, and Gary Shiu. *Phenomenology of a three-family standard-like string model*. Phys. Rev. D66, 066004 (2002), [hep-ph/0205252](#).
- [31] Mirjam Cvetic, Paul Langacker, and Gary Shiu. *A three-family standard-like orientifold model: Yukawa couplings and hierarchy*. Nucl. Phys. B642, 139–156 (2002), [hep-th/0206115](#).
- [32] Mirjam Cvetic, Ioannis Papadimitriou, and Gary Shiu. *Supersymmetric three family  $SU(5)$  grand unified models from type IIA orientifolds with intersecting D6-branes*. Nucl. Phys. B659, 193–223 (2003), [hep-th/0212177](#).
- [33] Mirjam Cvetic and Ioannis Papadimitriou. *More supersymmetric standard-like models from intersecting D6-branes on type IIA orientifolds*. Phys. Rev. D67, 126006 (2003), [hep-th/0303197](#).
- [34] Mirjam Cvetic, Tianjun Li, and Tao Liu. *Supersymmetric Pati-Salam models from intersecting D6- branes: A road to the standard model*. (2004), [hep-th/0403061](#).
- [35] Marianna Larosa and Gianfranco Pradisi. *Magnetized four-dimensional  $Z(2) \times Z(2)$  orientifolds*. Nucl. Phys. B667, 261–309 (2003), [hep-th/0305224](#).
- [36] Ralph Blumenhagen, Lars Görlich, and Tassilo Ott. *Supersymmetric intersecting branes on the type IIA  $T^6/\mathbb{Z}_4$  orientifold*. JHEP 01, 021 (2003), [hep-th/0211059](#).
- [37] Gabriele Honecker. *Chiral supersymmetric models on an orientifold of  $\mathbb{Z}_4 \times \mathbb{Z}_2$  with intersecting D6-branes*. (2003), [hep-th/0303015](#).
- [38] Gabriele Honecker. *Supersymmetric intersecting D6-branes and chiral models on the  $T(6)/(Z(4) \times Z(2))$  orbifold*. (2003), [hep-th/0309158](#).

- [39] D. Cremades, L. E. Ibanez, and F. Marchesano. *SUSY quivers, intersecting branes and the modest hierarchy problem*. JHEP 07, 009 (2002), [hep-th/0201205](#).
- [40] D. Cremades, L. E. Ibanez, and F. Marchesano. *More about the standard model at intersecting branes*. (2002), [hep-ph/0212048](#).
- [41] Christos Kokorelis. *Deformed intersecting D6-brane GUTs and  $N = 1$  SUSY*. (2002), [hep-th/0212281](#).
- [42] Christos Kokorelis.  *$N = 1$  locally supersymmetric standard models from intersecting branes*. (2003), [hep-th/0309070](#).
- [43] Edward Witten. *Comments on string theory*. (2002), [hep-th/0212247](#).
- [44] Igor R. Klebanov and Edward Witten. *Proton decay in intersecting D-brane models*. Nucl. Phys. B664, 3–20 (2003), [hep-th/0304079](#).
- [45] Mirjam Cvetic and Ioannis Papadimitriou. *Conformal field theory couplings for intersecting D-branes on orientifolds*. Phys. Rev. D68, 046001 (2003), [hep-th/0303083](#).
- [46] D. Lüst and S. Stieberger. *Gauge threshold corrections in intersecting brane world models*. (2003), [hep-th/0302221](#).
- [47] Ralph Blumenhagen, Dieter Lüst, and Stephan Stieberger. *Gauge unification in supersymmetric intersecting brane worlds*. (2003), [hep-th/0305146](#).
- [48] D. Cremades, L. E. Ibanez, and F. Marchesano. *Yukawa couplings in intersecting D-brane models*. JHEP 07, 038 (2003), [hep-th/0302105](#).
- [49] Boris Körs and Pran Nath. *A Stueckelberg extension of the standard model*. (2004), [hep-ph/0402047](#).
- [50] Noriaki Kitazawa. *Dynamical generation of mu-terms and Yukawa couplings in intersecting D-brane models*. (2004), [hep-th/0403278](#).
- [51] D. Cremades, L. E. Ibanez, and F. Marchesano. *Intersecting brane models of particle physics and the Higgs mechanism*. JHEP 07, 022 (2002), [hep-th/0203160](#).
- [52] D. Cremades, L. E. Ibanez, and F. Marchesano. *Towards a theory of quark masses, mixings and CP- violation*. (2002), [hep-ph/0212064](#).
- [53] Mirjam Cvetic, Paul Langacker, and Jing Wang. *Dynamical supersymmetry breaking in standard-like models with intersecting D6-branes*. Phys. Rev. D68, 046002 (2003), [hep-th/0303208](#).
- [54] Boris Körs and Pran Nath. *Effective action and soft supersymmetry breaking for intersecting D-brane models*. Nucl. Phys. B681, 77–119 (2004), [hep-th/0309167](#).
- [55] Jan Louis, Ilka Brunner, and Stephan J. Huber. *The supersymmetric standard model*. (1998), [hep-ph/9811341](#).
- [56] Dieter Lüst. *Intersecting brane worlds: A path to the standard model?* (2004), [hep-th/0401156](#).

[57] D. Lüst. *Intersecting brane worlds and their effective interactions.* Prog. Theor. Phys. Suppl. 152, 59–72 (2004).

[58] T. P. T. Dijkstra, L. R. Huiszoon, and A. N. Schellekens. *Chiral supersymmetric standard model spectra from orientifolds of Gepner models.* (2004), [hep-th/0403196](#).

[59] Ralph Blumenhagen. *Supersymmetric orientifolds of Gepner models.* JHEP 11, 055 (2003), [hep-th/0310244](#).

[60] Ralph Blumenhagen and Timo Weigand. *Chiral supersymmetric Gepner model orientifolds.* JHEP 02, 041 (2004), [hep-th/0401148](#).

[61] Ralph Blumenhagen and Timo Weigand. *A note on partition functions of Gepner model orientifolds.* (2004), [hep-th/0403299](#).

[62] L. R. Huiszoon. *D-branes and O-planes in string theory: An algebraic approach.*

[63] Lance J. Dixon, Jeffrey A. Harvey, C. Vafa, and Edward Witten. *Strings on Orbifolds.* Nucl. Phys. B261, 678–686 (1985).

[64] Lance J. Dixon, Jeffrey A. Harvey, C. Vafa, and Edward Witten. *Strings on Orbifolds 2.* Nucl. Phys. B274, 285–314 (1986).

[65] Duiliu-Emanuel Diaconescu, Michael R. Douglas, and Jaume Gomis. *Fractional branes and wrapped branes.* JHEP 02, 013 (1998), [hep-th/9712230](#).

[66] Duiliu-Emanuel Diaconescu and Jaume Gomis. *Fractional branes and boundary states in orbifold theories.* JHEP 10, 001 (2000), [hep-th/9906242](#).

[67] Mirjam Cvetic, Angel M. Uranga, and Jing Wang. *Discrete Wilson lines in  $N = 1$   $D = 4$  type IIB orientifolds: A systematic exploration for  $Z(6)$  orientifold.* Nucl. Phys. B595, 63–92 (2001), [hep-th/0010091](#).

[68] Matteo Bertolini. *Four lectures on the gauge-gravity correspondence.* (2003), [hep-th/0303160](#).

[69] G. Aldazabal, A. Font, Luis E. Ibanez, and G. Violero.  *$D = 4, N = 1$ , type IIB orientifolds.* Nucl. Phys. B536, 29–68 (1998), [hep-th/9804026](#).

[70] Matthias Klein and Raul Rabadan.  *$D = 4, N = 1$  orientifolds with vector structure.* Nucl. Phys. B596, 197–230 (2001), [hep-th/0007087](#).

[71] P. Griffiths and J. Harris. *Principles of Algebraic Geometry.* Wiley-Interscience, 1978.

[72] Michael R. Douglas. *The statistics of string / M theory vacua.* JHEP 05, 046 (2003), [hep-th/0303194](#).

[73] Gabriele Honecker and Tassilo Ott. *work in progress.*

[74] Matthias Klein and Raul Rabadan.  *$Z(N) \times Z(M)$  orientifolds with and without discrete torsion.* JHEP 10, 049 (2000), [hep-th/0008173](#).